Mantle-driven deformation of orogenic zones and clutch tectonics

Basil Tikoff, Ray Russo, Christian Teyssier and Andréa Tommasi

Geological Society, London, Special Publications 2004; v. 227; p. 41-64
doi:10.1144/GSL.SP.2004.227.01.03

Mantle-driven deformation of orogenic zones and clutch tectonics

BASIL TIKOFF[1], RAY RUSSO[2], CHRISTIAN TEYSSIER[3] & ANDRÉA TOMMASI[4]

[1]*Department of Geology and Geophysics, University of Wisconsin, Madison, WI 53706, USA (e-mail: basil@geology.wisc.edu)*

[2]*Department of Geological Sciences, Northwestern University, Evanston, IL 60208, USA*

[3]*Department of Geology and Geophysics, University of Minnesota, Minneapolis, MN 55455, USA*

[4]*Laboratoire de Tectonophysique, ISTEEM, CNRS/Université de Montpellier II, 34095 Montpellier cedex 5, France*

Abstract: Compatible deformation between the upper crust and upper mantle is documented for a variety of ancient and neotectonic settings, suggesting that these lithospheric layers are coupled. Areas of neotectonic deformation are also characterized by high seismic attenuation, indicating that the uppermost mantle is rheologically weak and flowing in these regions. The flow of the mantle, both lithospheric and asthenospheric, potentially drives deformation in continental orogenic zones. Three-dimensional models, controlled by bottom-driven mantle flow, are proposed for obliquely convergent, transcurrent and obliquely divergent plate margins. Our analysis indicates that the absolute, and not just relative, plate motions play a critical role in the orogenic cycle.

The Earth displays a radial compositional stratification, which results in depth-dependent variation in the strength of Earth materials (rheology). The rheology of each of these distinct lithospheric layers was quantified through the use of experimental deformation, and corroborated by geological field studies and microstructure analysis. A steadily accruing set of diverse data indicates that the Earth's continental crust is coarsely divisible into two mechanically distinct layers in continental regions: the upper crust and lower crust. The upper crust deforms by brittle or cataclastic mechanisms, while the lower crust deforms by crystal-plastic mechanism (Sibson 1977; Scholz 1988). The upper mantle underlying continental crust is also mechanically divisible into a more rigid lithospheric upper mantle and a more mobile, fluid-like asthenospheric mantle (Brace & Kohlstedt 1980). Modifications to these rheological estimates have been made, such as the recognition of the importance of micas in upper crustal deformation (Imber *et al.* 2001) or the effect of water in the mantle rheology (Kohlstedt *et al.* 1995).

The compositional and rheological heterogeneity of the lithospheric layers was used to infer horizontal décollement zones in the lithosphere, which results in decoupling of surface crustal blocks from underlying mantle (e.g. Oldow *et al.* 1990). If this scenario is true, it is an important obstacle for understanding how lithospheric motions and deformation relate to deeper Earth processes such as mantle convection: if there is no mechanical connection, plate tectonics is either independent or, at a minimum, does not have a simple relationship to mantle convection. This basic realization has recently emerged as one of the most fundamental problems of modern tectonics.

In this contribution, we synthesize geological, microstructural and geophysical datasets and propose a three-dimensional view of lithospheric deformation. In a variety of settings, upper crustal deformation (characterized by geological mapping and geodetic information) is remarkably similar to mantle deformation (shear-wave splitting data). Consequently, we infer that the layers are at least partially coupled in a process we call clutch tectonics (Tikoff *et al.* 2002). Alternatively stated, detachment zones are not ubiquitous in the ductile lower crust. Second, we use geophysical arguments to suggest that the uppermost mantle is composed of two distinctly different types: (1) rigid lithospheric mantle under oceanic crust and cratonic regions of continents; and (2) a more fluid, 'asthenospheric-like' mantle under mobile belts. Consequently, we use the term 'upper mantle' rather than lithospheric mantle or asthenospheric mantle, as the rheology of the upper mantle may depend on tectonic setting.

From: GROCOTT, J., MCCAFFREY, K. J. W., TAYLOR, G. & TIKOFF, B. (eds) 2004. *Vertical Coupling and Decoupling in the Lithosphere*. Geological Society, London, Special Publications, **227**, 41–64.
0305-8719/04/$15

The concept of plate tectonics has never worked particularly well in mountain belts: plates as lithospheric columns that remain intact through time do not exist in these settings. The observations suggest that crustal deformation is potentially tied in a direct way to underlying mantle movement (e.g. convection), through a series of subhorizontal, high-strain zones which act to partially attach adjacent lithospheric layers. We first present an overview of the observations, both geological and geophysical. We then present the clutch model to explain the observed phenomenon in the context of mantle-driven flow. Last, we investigate the importance of absolute plate motions for orogenic deformation.

Observations

Lithospheric deformation

The upper crust is the best-studied lithospheric layer in terms of deformation. Deformation is both aseismic and seismic, and the bulk rheology is mostly characterized by Coulomb behaviour. The deformation mechanisms for upper crustal deformation are cataclastic flow, pressure solution and dislocation creep. The translation and rotation of upper crustal blocks is well demonstrated by Global Positioning System (GPS) data. Internal strain of the upper crustal blocks is also recorded by GPS data, although the signal contains both transient elastic deformation of the crust and shallow mantle (i.e. seismic cycle) and permanent tectonic strain due to plate motions. Standard kinematic analysis of structural geological data allows one to constrain three-dimensional, finite deformation. Accurate average velocities (and strain rates) are obtainable with this technique, provided that the timing of deformation is well bracketed (e.g. Christensen *et al.* 1989; Dunlap *et al.* 1997).

The lack of normal seismicity indicates that the lower crust ($\gtrsim$15 km depth) is significantly different rheologically and/or compositionally from the upper crust. Geological observations on exposed lower crustal sections suggest a bulk felsic composition for the lower crust, consistent with seismic velocity (i.e. V_P/V_S) studies on *in situ* sections (Christensen & Mooney 1995). Layering in the lower crust is generally subhorizontal to shallowly dipping, observed both geologically and geophysically. In addition, large sections of the exposed lower crust contain nappes and sheath-fold structures, indicating large amounts of plastic strain (e.g. Goscombe 1992). These structures are important as they imply that the lower crust is pervasively deformed.

Mantle deformation can be deduced from shear-wave splitting datasets in a variety of orogenic zones. The result of seismic shear waves travelling through anisotropic media is shear-wave splitting, similar to optical birefringence, in which the incoming shear wave is split in two quasi-orthogonal waves that travel at different speeds (see reviews by Silver 1996; Savage 1999). The time lag between the two waves is controlled by the intrinsic anisotropy of the medium, which depends on the intensity of the lattice preferred orientations, and by the thickness of the anisotropic layer. Typical splitting delays in neotectonic regions are $\sim$1–2 s. Most of the observed shear-wave splitting for teleseismic travel paths is considered to arise in the upper mantle, extending down to the 410 km seismic discontinuity. While crustal rocks contain large intrinsic anisotropies, the relative thinness and the variability of the deformation fabrics of the continental crust rule it out as a major source of shear-wave splitting. Barruol & Kern (1996) have shown that the crust typically contributes $\sim$0.1–0.2 s of splitting, with 0.5 s delays in extreme cases. Moreover, kilometre-scale exposures of upper mantle rocks show a strong fabric, consistent with the interpretation of pervasive deformation in these settings (e.g. Christensen 2002).

Mantle fabric

Olivine LPO and shear-wave splitting. The observed shear-wave splitting in mobile belts is presumed to result primarily from the lattice preferred orientation (LPO) of olivine, the most abundant mineral in the upper mantle. Olivine displays anisotropic elastic properties (Abramson *et al.* 1997), with compressional seismic waves travelling 25% faster when parallel to the fast [100] axis relative to the slow [010] axis. Shear-wave propagation is also affected by this elastic anisotropy. The highest anisotropy (*c.* 18%) is recorded by waves propagating in a direction intermediate between the [100] and the [001] crystallographic axes, and fast split shear waves are polarized parallel to the [100] axis of olivine. The anisotropy of olivine is relatively low compared to that of some other silicate minerals, such as biotite. The large delay times recorded by shear-wave splitting are due to the thickness of the mantle sampled by the seismic waves, rather than to the inherent anisotropy of the material. Shear-wave splitting requires that the olivine crystals display coherent orientations (i.e. strong LPO) over large distances in the upper mantle (>50 km). Therefore, dislocation creep must be active in at least the upper 250–300 km of the mantle, since diffusion creep does not produce an LPO. This inference is consistent with experimental deformation, which suggests that dislocation creep occurs in olivine aggregates at upper mantle temperatures and pressures (e.g. Zhang & Karato 1995).

Seismic anisotropy, such as shear-wave splitting, results from the deformational fabric of mantle rocks. Shear-wave splitting observations provide information about deformation in the mantle, allowing us to conduct structural geology analysis of the mantle in these settings. The relation between deformation and olivine LPO is critical to our interpretation of seismic anisotropy data in terms of upper mantle kinematics. Comparison between shape preferred orientation of olivine and spinels in a large number of naturally deformed mantle rocks indicates that the olivine [100] axis usually tends to concentrate at low angle to the lineation. The [010] axis either concentrates at high angles to the foliation or forms a girdle normal to the lineation (Ben Ismail & Mainprice 1998). This LPO suggests a dominant activation of the (010)[100] and (001)[100] slip systems in olivine for deformation under upper mantle conditions (Tommasi *et al.* 2000). Analysis of olivine LPO evolution in high-temperature deformation experiments, as well as in polycrystalline plasticity models, provides some further constraints on this relation.

Laboratory experiments. Deformation experiments of both olivine single crystals and polycrystalline aggregates under high-temperature, high-pressure conditions provide valuable constraints on: (1) how the activation of the various slip systems, and hence the LPO, is affected by physical parameters such as temperature, water and oxygen fugacity; and (2) how olivine LPO reflects the flow kinematics and/or finite strain. Flow experiments on olivine crystals, under predicted upper mantle pressure and temperature conditions, show that the dominant slip system is most likely (010)[100], followed by the (001)[100] system. Under high water or oxygen fugacity conditions, slip on the latter system tends to dominate (Bai *et al.* 1991; Mackwell *et al.* 1985). On the other hand, low-temperature experiments show a dominant activation of glide on the [001] direction (Phakey *et al.* 1972). Analysis of olivine LPO in naturally deformed peridotites shows that upper mantle deformation is generally accommodated by slip on both (010)[100] and (001)[100] systems, with dominance of the former. Moreover, glide in the [001] direction is only significant during low-temperature deformation associated with the emplacement of mantle slabs into the crust (Tommasi *et al.* 2000).

In simple shear experiments under high-T conditions, deformation fabrics yield seismic anisotropy with an LPO characterized by a concentration of olivine [100] axes parallel to the elongation direction (Fig. 1). The fabrics obtained in the various experiments deviate, however, with respect to the orientation of [010] axes and [001] axes. In plane-strain experiments, Zhang & Karato (1995) found point maxima for the crystallographic [010] axes and [001] axes of olivine approximately perpendicular to the shear plane and approximately perpendicular to the shear direction within the shear plane, respectively. In contrast, Bystriky *et al.* (2000) report girdles of crystallographic [010] axes and [001] axes of olivine for torsion experiments (Fig. 1). Both types of LPO are common in mantle xenoliths and mantle sections of ophiolites (Ben Ismail & Mainprice 1998).

We tentatively suggest that the Zhang & Karato (1995) data represent slightly higher temperatures (1300 °C v. 1200 °C) than the experiments of Bystriky *et al.* (2000). The LPO patterns are the same, only the development is faster for the Zhang & Karato experiments because of stronger dynamic recrystallization. This inference is broadly consistent with the results of Carter & Avé Lallemant (1970), in which point distributions of crystallographic axes and activation of (001)[100] occurred at the highest-temperature conditions. A major difference, however, between the Zhang & Karato (1995) and Bystriky *et al.* (2000) experiments is the type of strain. The experiments of Bystriky *et al.* (2000) are simple shear, whereas the experiments of Zhang & Karato (1995) contained a component of coaxial deformation parallel to the shear direction (reported in Zhang *et al.* 2000). This coaxial component, in addition to the possible formation of extensional shear bands, will lower the angle between the long axis of the finite strain ellipse and the shear plane. Therefore, in both experiments, the [100] axes are parallel to the long axis of the finite strain ellipsoid.

Numerical experiments. The development of LPO in olivine aggregates has also been addressed using forward modelling. Several approaches have been utilized, including visco-plastic self-consistent (Wenk *et al.* 1991; Wenk & Tome 1999; Tommasi *et al.* 1999), stress equilibrium (Chastel *et al.* 1993) and kinematic constraint (Ribe & Yu 1991; Kaminski & Ribe 2001) models. These LPO predictions using these various approaches and their application to the

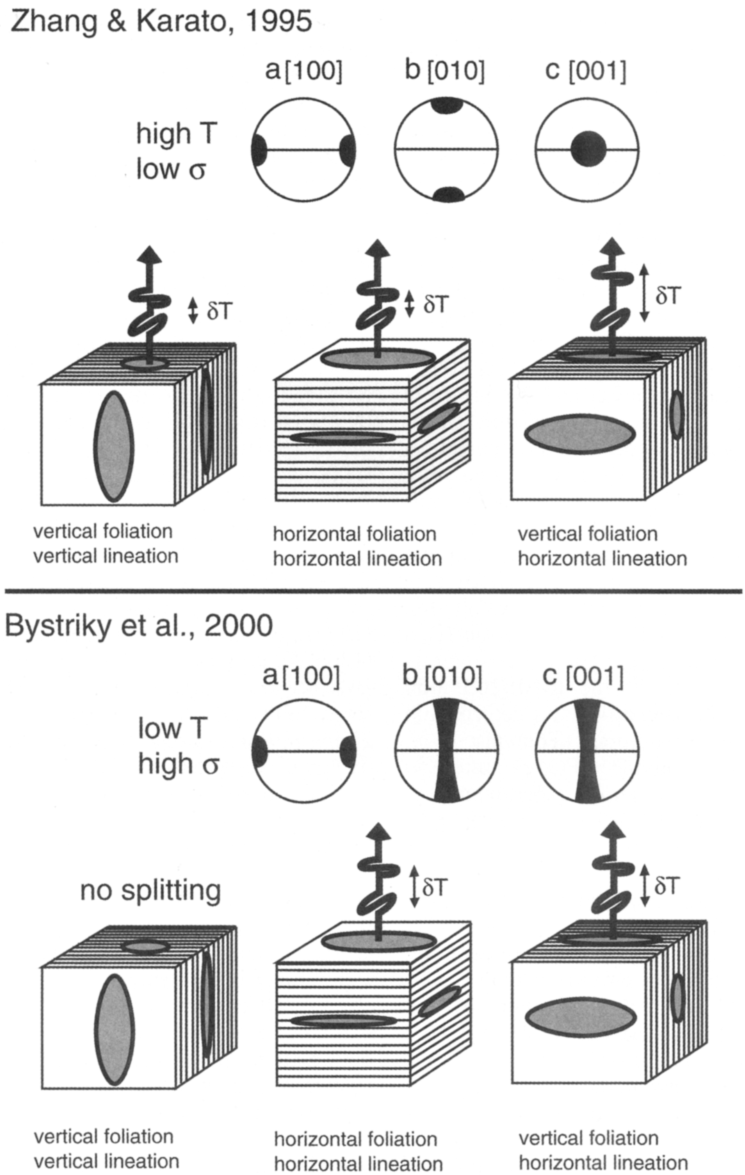

Fig. 1. Olivine microstructures produced under different deformation boundary conditions. The experiments of Zhang & Karato (1995), potentially applicable to higher-temperature deformation, produce point maxima. The results of Bystriky *et al.* (2000) indicate a point maximum for the [100] axis and a girdle distribution for the [010] and [001] axes. The resultant shear-wave splitting, in either case, depends on the orientation of the LPO since SKS waves have a near-vertical incidence. In either case, vertical foliation and horizontal lineation produces strong shear-wave splitting.

prediction of seismic properties are reviewed in Tommasi *et al.* (2000).

In general, classical polycrystalline plasticity models (in which deformation is accommodated by dislocation glide only) predict that the olivine [100] axes tend to parallel the maximum finite elongation direction and that the [010] axis will tend to align normal to the foliation. In more complex three-dimensional flow types, the olivine [100] axis tends to align with the long axis of the finite strain ellipsoid (Tommasi *et al.* 1999). These results hold true specifically for transpressional and transtensional deformation. These deformations are unusual because a switch in lineation orientation (transpression) or foliation orientation (transtension) can occur for either: (1) different angles of oblique convergence/divergence; or (2) increasing strain at a single angle of oblique convergence/divergence (Tikoff & Greene 1997).

Analysis of olivine LPO development in polycrystalline plasticity models also highlights that LPO intensity does not depend linearly on finite strain (Tommasi *et al.* 2000). At shear strains of 1–2, clear LPOs are already formed. This result is in agreement with LPO evolution in simple-shear experiments, which shows a fast evolution up to shear strains of 1 or 2 and then maintenance of a steady-state fabric (Bystriky *et al.* 2000). Comparison between model predictions and LPO intensity in naturally deformed rocks also suggests that LPO only records part of the total strain accommodated by the rock.

Mantle viscosity: the significance of seismic attenuation

The degree of observed shear-wave splitting for mantle paths attains a global average of just over 1 s and is as high as 2.7 s (Marson-Pidgeon & Savage 1997). These values imply that, for nominal values of intrinsic anisotropy derived from laboratory studies, coherent deformation fabrics in the upper mantle of the order of 100–200 km thick exist (Silver 1996). The vertical extent of this pervasive deformation has given rise to an important debate (e.g. Vinnik *et al.* 1989*a*, *b*; Silver & Chan 1991). Is this pervasive fabric contained in a highly viscous lithosphere, or does the shear splitting signal arise from a plastically flowing asthenosphere? Given normal geotherms, especially for tectonically active regions, 200 km of coherently deformed material may include an anisotropic asthenospheric source layer as well as the 'frozen' fabrics of the overlying lithosphere. If the anisotropic layer is strictly asthenospheric, then this ductile layer is potentially a zone of weak viscous coupling, or even decoupling, between the lithosphere and the deeper mesosphere. Seismic attenuation has the potential to resolve this issue.

Seismic attenuation is due either to scattering of seismic energy along the wave path or to intrinsic attenuation of seismic energy caused by conversion of displacive energy into thermal energy (thermal dissipation). Normally, such loss is higher for shear waves than for compressional waves. Therefore, a comparison of the frequency contents of S waves relative to P waves can be made to be diagnostic of attenuation in a quantitative way. This measure is referred to as 'Q' for quality factor. Q is a dimensionless number that is inversely related to attenuation. For Earth materials that are near their solidus, Q is normally in the 100–200 range. Q for rigid lithosphere of oceanic slabs is 800 or more (e.g. Okal & Talandier 1997). Consequently, Q measurements are useful indicators of rheology.

Attenuation along paths restricted to oceanic lithosphere, excluding spreading ridges, is low (high Q). In cratonic regions, presumably underlain by thick, cold, high-velocity roots, seismic attenuation is also low. For these two areas, oceanic lithosphere and cratonic regions, the upper mantle is inferred to be relatively rigid (e.g. Lay & Wallace 1995). In contrast, for seismic travel paths that include oceanic asthenosphere or upper mantle beneath most actively deforming regions, attenuation is high (low Q). Seismologists typically interpret such regions to be near solidus temperatures and rheologically weak or even flowing. The presence of small percentages of partial melt (1–2%) is often discussed for these regions (e.g. Roth *et al.* 1999). The crustal contribution to attenuation is minimal, due to the short path lengths for near-vertical, teleseismic rays.

The combination of shear-wave splitting measurements and seismic attenuation observations can constrain the ultimate source of mantle deformation. For example, one can discriminate between active mantle flow in a rapidly deforming layer and presence of a relict fabric in a lithospheric volume that is not deforming actively. In both cases, we might observe a strong, consistent shear-wave splitting pattern across an area. In the flowing asthenosphere case, however, attenuation is high (low Q). In contrast, attenuation will be low for the preserved old lithosphere fabric. If both strong lithospheric and asthenospheric fabric are present in an area, Q measurements may still discriminate between the two given the proper set of earthquake sources and seismic stations.

The lateral extent of long delay-time shear-wave splitting measurements in active tectonic regions suggests that the relatively narrow plate boundaries observed on the surface in continental regions correspond to very wide plate boundaries in the upper mantle (Russo *et al.* 1996; Klosko *et al.* 1999). Assuming that this upper mantle material is flowing by crystal-plastic processes, lateral displacements are potentially controlled by variations in lithospheric thickness. Convergent boundaries, by definition, result from the juxtaposition of two different lithospheres. Consequently, mantle flow in these regions is affected by thickness variations in both lithospheres.

Lithosphere/asthenosphere connections

Cratons and asthenosphere

Oceanic lithosphere contains a seismically detectable low-velocity zone inferred from dispersion of surface waves in ocean basins. Continental lithosphere, in contrast, lacks a low-velocity zone. Additionally, tomographic observations indicate that Precambrian cratonal regions are underlain by high-velocity regions extending to 300 km or more in some cases (e.g. van der Lee & Nolet 1997). These observations imply that: either (1) cratonic regions are coupled to large-scale mantle circulation (and hence there is no asthenospheric shear zone at their bases); or (2) any decoupling layer beneath cratons is much deeper than decoupling beneath ocean basins ($\sim$160 km) and is essentially different in seismic character. Compositional differentiation whereby a buoyant, strong residuum of mantle material forms the roots beneath ancient continental cores can account for the thicknesses, observed seismic velocity and apparent unsubductibility of the cratonic mantle lithosphere (e.g. Jordan 1975; Carlson 1995). These roots may also explain that asthenosphere does not develop at normal depths beneath these regions. If 'asthenospheric' shear zones do exist beneath cratons, the thermal regime, pressure regime and composition are significantly different from those of oceanic asthenosphere. Therefore, significantly different rheology and strain rates are expected. Given the possible viscosity increases, the effects of these differences on rheology are difficult to constrain quantitatively.

Insight into the deformation regime beneath cratons can be garnered from mantle xenoliths brought to the surface at kimberlite pipes. Kennedy *et al.* (2002) note that mantle peridotites that demonstrably come from the deep subcratonic mantle are divisible into two groups: (1) coarse-grained protogranular peridotites, and (2) fine-grained porphyroclastic peridotites. The latter are pervasively deformed at higher strain rates than the former and are only found at lower lithospheric levels ($\sim$150–200 km) as determined from thermobarometry. Kennedy *et al.* (2002) infer that deformation recorded by the porphyroclastic peridotites is more recent than the last-known deformation (Phanerozoic) visible at the Earth's surface. What younger deformation can these fabrics possibly represent? These authors argue that the porphyroclastic peridotites found in the kimberlite xenoliths are samples of the lithosphere–asthenosphere decoupling shear zone beneath cratons, thus explaining their high strain rate deformation (Kennedy *et al.* 2002). If this is correct, then shear at the base of cratons occurs deeper and without the associated seismic low-velocity zone found in oceanic asthenosphere. There are several potential problems with this interpretation, including the lack of independently confirmed textural ages of the fabrics and the cause of initial formation.

Finally, we note that the 'high' strain rate inferred from these xenoliths may be only relatively high, in comparison to those expected in oceanic asthenosphere. Thus, the very low seismic attenuation typically observed in cratonic regions, and the absence of a seismically defined low-velocity zone, could both be consistent with a deep, lower strain rate acting within a decoupling zone beneath cratons. Moreover, subcratonic mantle shear zones have sufficient time to acquire such a fabric. In contrast, the fabrics developed in oceanic asthenosphere are limited by the temporal existence of unsubducted young oceanic lithosphere ($<$170 Ma).

Lithospheric v. asthenospheric fabrics

Oceanic settings. The relation between lithospheric and asthenospheric upper mantle 'deformation' fabrics is clearest in the Pacific Ocean basin. Pn waves (Moho head waves, which are a regional seismic phase that travels along the Moho for most of its propagation) travelling just below the oceanic crust exhibit strong azimuthal anisotropy (e.g. Hess 1964; Raitt *et al.* 1969). The fast trends for these phases align with the mineralogical fabric imparted at spreading ridges when magma freezes while undergoing shear at the base of forming lithosphere (Fig. 2). This shear flow aligns upper mantle olivine [100] axes parallel to the spreading direction. In the older portions of the Pacific basin, this alignment results in fast Pn trends parallel to fracture zones. In contrast, a small but growing dataset of teleseismic shear-wave splitting indicates that this anisotropy is not detected. Instead, a strong asthenospheric signal yields fast shear polarization directions parallel to the current absolute plate motion (hotspots assumed fixed) of the Pacific plate (Fig. 2; Russo & Okal 1998; Wolfe & Silver 1998; Klosko *et al.* 1999). Surface wave analyses of the ocean basins show that upper mantle azimuthal anisotropy is generally closely related to lithospheric absolute plate motions, particularly in the Pacific basin (Nishimura & Forsyth 1988, 1989; Montagner &

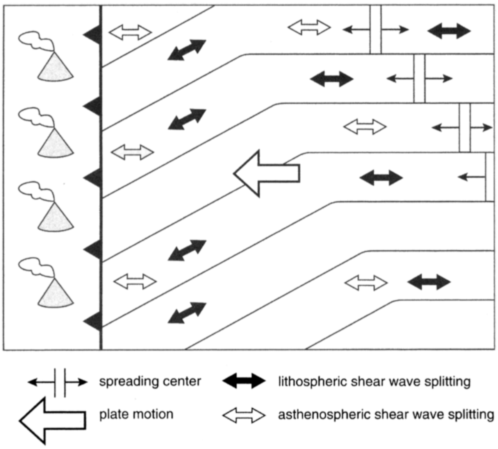

Fig. 2. Shear-wave splitting in oceanic material, in map view. Lithospheric fabric, frozen in from asthenospheric flow at the spreading centre, is parallel to the fracture traces. Asthenospheric fabrics are parallel to the current direction of plate motion in a fixed mantle reference frame. These two diverge if the motion of the plate has changed, such as for oceanic material older than 43 Ma in the Pacific region.

Tanimoto 1990, 1991). Pn anisotropy and shear-wave splitting are generally not parallel in the Pacific basin, since the fracture zones in lithosphere older than around 43 Ma do not parallel today's absolute plate motion direction.

These data have been interpreted to signal the operation of simple asthenospheric flow beneath the Pacific plate (Nishimura & Forsyth 1988, 1989; Montagner & Tanimoto 1990, 1991; Russo & Okal 1998; Wolfe & Silver 1998; Klosko *et al.* 1999; Vinnik *et al.* 1989*a*, *b*). As the plate moves rapidly towards western Pacific subduction zones, shear is imposed by the underlying asthenosphere. This shear transfer is presumed to occur in the low-velocity zone, producing effective decoupling or weak viscous coupling between the plate and the upper mantle below the asthenosphere.

Fabric in the lithospheric mantle is not properly a lithospheric deformation fabric in the sense we have been using elsewhere in this chapter. It records a 'frozen' asthenospheric flow that formed at a spreading centre, and not lithospheric deformation. This is distinct from the current fabric in the asthenosphere, which formed since 43 Ma when the Pacific plate's motion changed. Thus, asthenospheric fabric beneath oceanic lithosphere is potentially erased in an oceanic setting. This 'erasing' may not occur in continental lithosphere–asthenosphere fabrics (Vauchez & Garrido 2001).

Continental settings. The more complicated horizontal layering of the continental lithosphere–asthenosphere system produces a different response to tectonic loading. Lateral loading has the three end-member cases of contractional, extensional and wrench loading. Each type of loading results in a different mechanical response: thrusting, viscous shortening, thickening and buckling (contraction); normal faulting, crustal boudinage and extensional necking (extension); and strike-slip faulting and ductile shear flow (wrench). However, the observational basis for comparing lithospheric and asthenospheric fabrics in continental lithosphere is lacking for two reasons. First, discrimination between lithosphere and asthenosphere in continental settings requires more sophisticated seismic measurements than standard travel time inversion. Second, the heterogeneity of the continental lithosphere makes resolution of the lithosphere–asthenosphere difficult. For example, tomography might reveal what appears to be a cold, stiff lithosphere overlying a hotter asthenosphere, but a compositional difference could just as well explain the two velocity anomalies. Attenuation measurements for phases following specific paths, such as Pn or Sn, can afford a basis for discrimination between layers that are rheologically strong or weak. However, interpretations are tenuous without earthquakes or well-placed stations. Pn (Moho head) waves appear not to propagate in geologically complex regions, although the exact reasons are unknown. This leads to an unsatisfying guess about the actual rheology at depth.

Regions that are tectonically active are least likely to have thick lithosphere (e.g. Plomerova *et al.* 2002), and thus measurements of core phase shear-wave splitting (e.g. SKS) are likely to sample asthenospheric anisotropy only. Even if the lithospheric signal is clearly discriminated from the asthenospheric signal, the paths of shear waves most commonly used for splitting analyses cross both, yielding an inherent uncertainty in the source(s) of any splitting observed at the surface. In a few continental regions, systematic variability in splitting parameters was detected and interpreted as a function of the arrival azimuth of the shear wave at the station (Savage & Silver 1993). Such variability is most often ascribed to the presence of two layers of different anisotropy, each of which splits the arriving shear waves. Interpretations of such data have so far been restricted to assuming that the topmost layer is the lithosphere (or crust) and the lower layer is the asthenosphere (or possibly the mantle lithosphere) (Savage & Silver 1993). The inherent uncertainty arises from the mismatch between two assumed layers of anisotropy, although there are four potentially different anisotropic layers to consider (upper crust, lower crust, mantle lithosphere and asthenosphere). As the crustal component contributes only 0.1–0.2 s of splitting because of its limited extent (Barruol & Kern 1996), the mantle layers should dominate the splitting. Where two-layer anisotropy is detectable, different fabrics must be stacked vertically, which requires strong vertical deformation gradients.

An advanced type of study involves simultaneous determinations of Pn velocity and anisotropy (Hearn 1996, 1999; Mele *et al.* 1998; Calvert *et al.* 2000). Pn can provide a useful constraint on the question of lithosphere–asthenosphere fabric differences. This phase preferentially samples the uppermost mantle, which is probably lithosphere even in active tectonic environments with thin lithospheres. Estimates of azimuthal anisotropy from Pn can be directly compared to core phase shear-wave splitting measurements, which generally sample the entire upper mantle, including the lithosphere–asthenosphere package.

Furthermore, seismic investigations require a trade-off between Pn anisotropy and lateral velocity (Mochizuki *et al.* 1997), compromising fine resolution. However, careful studies show interpretable results (Hearn 1996). Good Pn anisotropy is comparable to shear-wave splitting results, and can potentially determine whether the splitting is dominated by the uppermost mantle portion of the phases' travel paths or deeper portions thereof. If the Pn and splitting anisotropies are similar, the vertical distribution of anisotropy must be fairly constant. Moreover, if mantle lithosphere and asthenosphere are both present, the fabrics of each must be similar. Alternatively, if the anisotropies differ, it is likely that the lithospheric fabrics differ from asthenospheric fabrics.

In many regions, comparison of Pn- and splitting-derived anisotropies indicates that the uppermost mantle fabrics are very similar to the integrated fabrics delineated by shear-wave splitting. The tectonic environments in which this is true include the region around the San Andreas fault and the western portion of the Great Basin (Hearn 1996), the Cascades region of western Washington state (compare Hearn 1996 and Bostock & Cassidy 1995), the central Appenines (Margheriti *et al.* 1996; Amato *et al.* 1997; Mele *et al.* 1998; Hearn 1999) and the Aegean region (compare Hearn 1999 and Hatzfeld *et al.* 2000). Thus, regions dominated by contraction, extension and wrenching all include large regions where uppermost lithosphere and deeper lithosphere–asthenosphere packages have similar fabrics in the rheologically layered continental stack. Note that the correspondence between Pn and splitting anisotropy is not always close, even in the small portion of the continents that have been carefully studied. Thus, there is the possibility for differential vertical deformation between the lithosphere and asthenosphere. Regions that document disagreement between the two sets of observations include the Sierra Nevada region and central valley of California, the Idaho Batholith–Snake River Plain region, the Rio Grande rift area (Hearn 1996), the Tyrrhenian Sea (Mele *et al.* 1998; Hearn 1999) and the Rhine Graben (Vinnik *et al.* 1994; Enderle *et al.* 1996; Plomerova *et al.* 1998; Hearn 1999).

Coincidence of crustal deformation and mantle fabric

Ancient orogens

In a variety of settings, upper crustal and mantle deformation are remarkably similar. In all cases, mantle deformation is constrained by shear-wave splitting data. The deformation of the upper crust is recorded by a variety of features. In ancient orogens, the record of upper crustal deformation is typically that of the orientation of structures. The Superior Province of North America and the Kaapvaal craton of South Africa both show shear-wave splitting parallel to the dominant Archaean-age structure of the region (e.g. Silver 1996). Likewise, parallelism between Late Proterozoic collisional fabrics in the mid to lower crust and SKS splitting data are also recorded in the Ribeira–Aracuai belt of SE Brazil (Vauchez *et al.* 1994; James & Assumpcao 1996). Palaeozoic orogenies show similar patterns. Barruol *et al.* (1997) show that the shear-wave splitting parallels the structural trend of the Appalachian–Caledonian–Hercynian belt. Consequently, for this and all the above cases, the current shear-wave splitting data represent a 'frozen' signal in the mantle lithosphere from orogenesis.

Vauchez *et al.* (1997) further suggest that the reactivation of orogenic belts in continental break-up is a result of this 'frozen' anisotropy in the mantle lithosphere. Polycrystalline plasticity models show that a mechanical anisotropy, due to olivine LPO frozen in the lithospheric mantle since the last orogenic episode, may induce a directional strain softening in the lithospheric mantle and control the localization of continental break-up (Tommasi & Vauchez 2001).

Neotectonic orogens

Neotectonic zones allow more quantitative conclusions to be drawn on the relation between the development of mantle fabric and crustal deformation. A wide range of neotectonic areas have been studied, ranging from transcurrent domains (Trinidad) to convergent ones (Himalayas). The San Andreas system and New Zealand represent intermediate situations, characterized by increasing amounts of convergent motion in obliquely convergent settings (Fig. 3).

Despite the wide range of tectonic settings, there are clear similarities in all of the above examples. Regardless of the angle of relative plate motion, the fast polarization direction of the shear-wave splitting is often at a small angle to the plate boundary. This is particularly clear in the obliquely convergent boundary in New Zealand (Fig. 3; Klosko *et al.* 1999; Molnar *et al.* 1999). The stations displaying the highest delay times show a fast shear wave polarized at $\sim$10–15 degrees from the trace of the Alpine fault. As one moves away from the plate boundary, the magnitude of the time delay decreases and the directions are oriented at higher angles to the Alpine fault. This observation indicates that some rotation in the orientation of LPO occurs as a result of finite strain gradients. Patterns of shear-wave splitting show ubiquitous rotation of splitting directions near strike-slip faults (San Andreas fault, California; El Pilar fault, Venezuela) in obliquely convergent systems. This observation suggests that zones of strain localization in the upper crust correspond to zones of strain localization in the upper mantle (e.g. Molnar 1992). In the Himalayas, fast shear-wave polarizations are only parallel to the trend of the belt close to the major strike-slip faults (Fig. 4; Lave *et al.* 1996). The general orientation of shear-wave splitting subparallel to the plate boundaries suggests: (1) rotation of the finite strain ellipse to an orientation parallel to the boundary; or (2) lateral flow along the margin (plane transpression of Tommasi *et al.* 1999).

Interpretation of the data

Holt (2000), using geodetic data from Tibet, calculated maximum shear strain rate planes. One of these planes is typically subparallel to the observed shear-wave splitting. Three different approaches were tried in South Island, New Zealand. Moore *et al.* (2002) utilized the orientation of the present velocity field and assumed that the deformation had accumulated for $\sim$6.5 Ma with this velocity field. The resultant deformation fits well with the observed shear-wave splitting. Little *et al.* (2002) calculate surface deformation using deformed, crustal-scale markers, and also find a very good correlation to inferred mantle deformation. In general, the surface deformation and shear-wave splitting data are consistent in extent and magnitude. It is not yet clear how to interpret this coincidence. There are at least two possibilities: (1) the mantle and the crust are coupled (McKenzie & Jackson 1983; Molnar 1992; Teyssier & Tikoff 1998); or (2) similar boundary conditions apply to the upper crust and upper mantle (Holt 2000). A third possibility, simple asthenospheric flow below the continents (e.g. Silver 1996), does not apply to orogenic zones. An exception to the last possibility is the proposed flow of asthenosphere under the Basin and Range of the western United States (e.g. Silver & Holt 2002).

The possibility that both lithospheric layers respond independently to side-driven boundary conditions (e.g. Holt 2000) is unlikely for a variety of reasons. First, the upper crust, as an individual lithospheric layer, is unlikely to transmit the stresses from the plate boundary to the interior of Asia. This is particularly true for the Himalayas given the existence of multiple lithospheric-scale suture zones bounding the collisional terranes, which would act as zones of strain localization. Second, Giorgis *et al.* (2004) document the coincidence in upper crustal deformation and mantle deformation associated with vertical-axis rotations in dominantly transcurrent environments. They document that bottom-driven models, compared to side-driven models, better describe the amount of vertical-axis rotation relative to the orientation of shear-wave splitting. The most significant, however, is the nature of mechanical instabilities within independently deforming layers. The thin and laterally extensive geometry of the lithospheric plates allows for only a few styles of deformation in response to a horizontal end load, such as buckling or boudinage (e.g. Burg *et al.* 1994 for the Himalayas). These types of mechanical instabilities cause localization of strain, which leads to discontinuous deformation. However, geodetic surveys of most orogenic zones indicate that upper crustal flow is broadly continuous (e.g. Beavan & Haines 2001 for the South Island of New Zealand). Consequently, it is unlikely that the upper crust deforms independently of the rest of the lithosphere.

An equally viable alternative is that the layers are in mechanical communication. This requires that the lower crust, and other presumed weak lithospheric horizons in the lithosphere, act to partially couple the upper crust and lithospheric

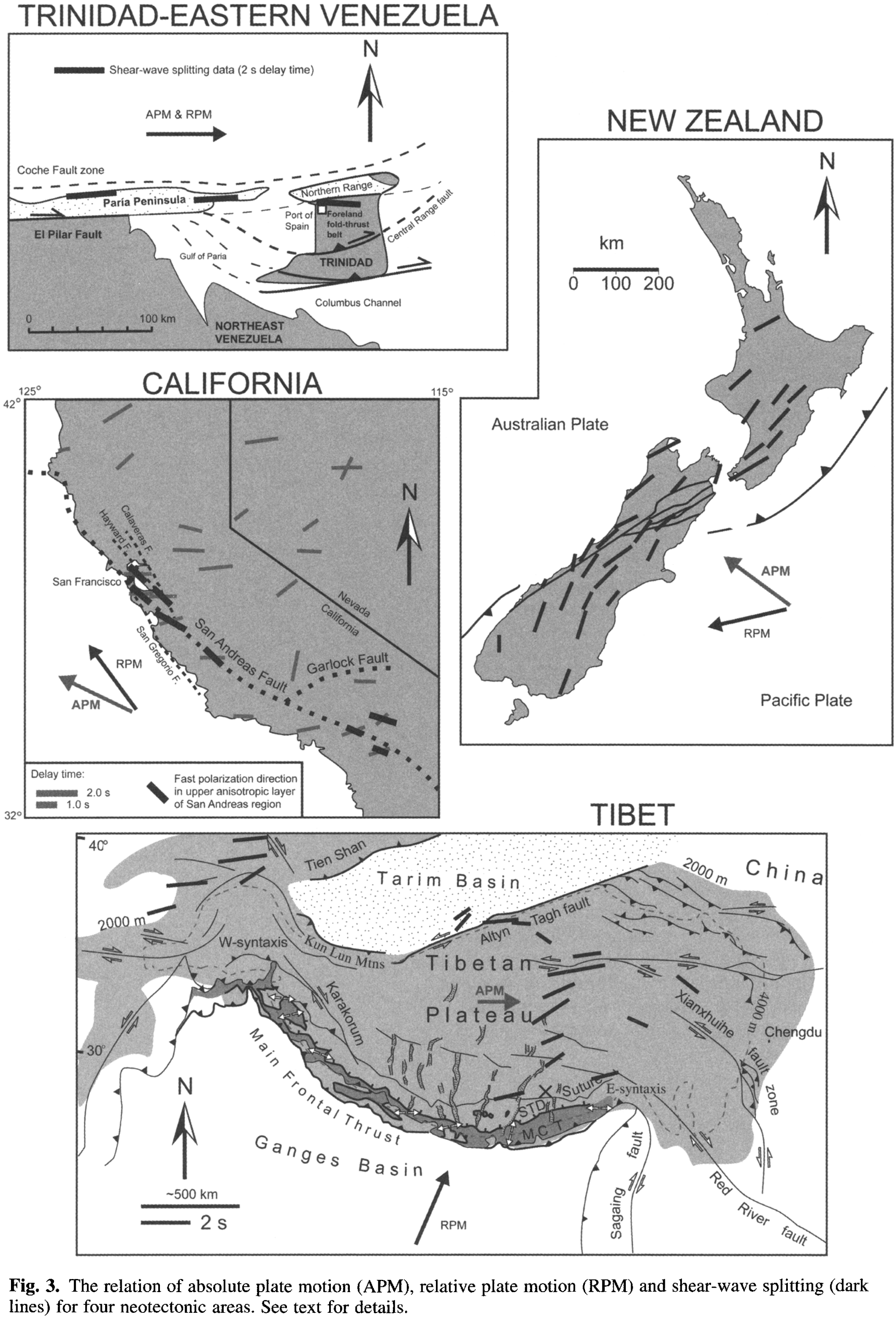

Fig. 3. The relation of absolute plate motion (APM), relative plate motion (RPM) and shear-wave splitting (dark lines) for four neotectonic areas. See text for details.

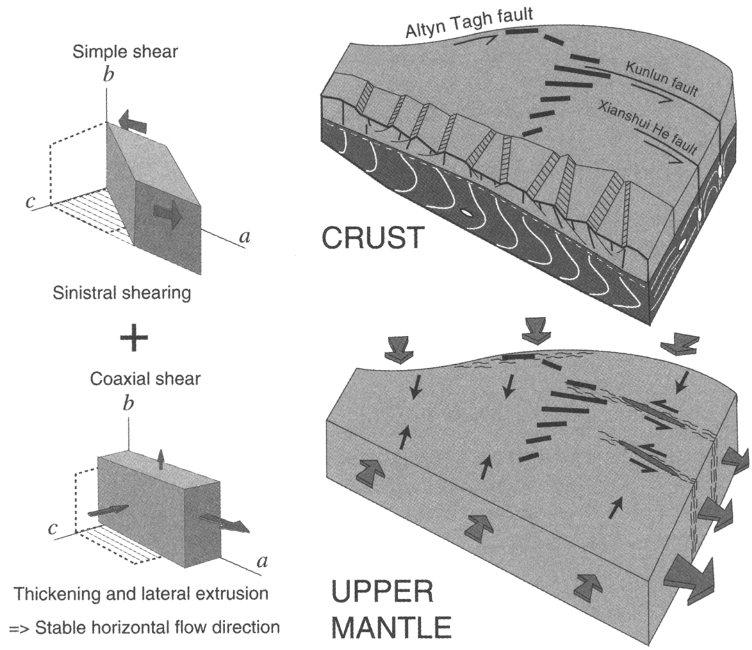

Fig. 4. Cartoon of lithospheric deformation in Tibet. Dark lines indicate the orientation and magnitude (length) of shear-wave splitting measurements. The short, wavy lines indicate zones of ductile shearing. Crustal deformation is characterized by normal faulting and strike-slip faulting, in addition to contractional structures. Mantle deformation, inferred from shear-wave splitting, indicates components of sinistral simple shear, concentrated near strike-slip faults, and coaxial extrusion (left side of diagram – shown with kinematic axes *a*, *b* and *c*). The coincidence of crustal deformation, inferred from geodetic motion in addition to geological structures, with the mantle deformation indicates that the lithospheric layers are coupled.

mantle layers. We explore this option in the next section (Clutch Tectonics).

A major limitation: strain history

Little *et al.* (2002) suggest that the geological history is potentially recorded in seismic anisotropy. Using two markers that were offset by the Alpine fault in South Island of New Zealand, the Junction magnetic anomaly and the Moonlight fold belt, the finite strain was modelled for upper crustal deformation assuming a transpressional deformation model. The calculated upper crustal deformation is in very good agreement with the shear-wave splitting. While this approach has the disadvantage of the assumption of originally linear markers, it has the advantage of addressing the geological history. Little *et al.* (2002) demonstrated that the upper crustal deformation was probably not constant with time, consistent with plate motion reconstructions. Therefore, it is potentially incorrect to determine the currently active deformation (e.g. geodetic data) and then integrate the data over some time to calculate the shear-wave splitting. Because shear-wave splitting results from a fabric, it is critical to incorporate the geological history of the plate boundary.

Clutch tectonics

We hypothesize that deformation in the crust and mantle are similar because these lithospheric layers are mechanically connected. Therefore, either displacements initiate in the upper crust and move downward (top-driven system) or displacements initiate in the mantle and move upward (bottom-driven) (Fig. 5). The zone that connects the top to the bottom is called a clutch zone, by analogy to the clutch of an automobile (Tikoff *et al.* 2002). A clutch allows mechanical continuity between the independently operating wheels and engine. Clutch zones, when present, have a different shear sense for top-driven or bottom-driven systems (Fig. 5c v. 5d). While the concept of top-driven systems was investigated for extensional deformation (e.g. Axen *et al.* 1998), bottom-driven systems must be the general rule in orogenic zones if tectonic

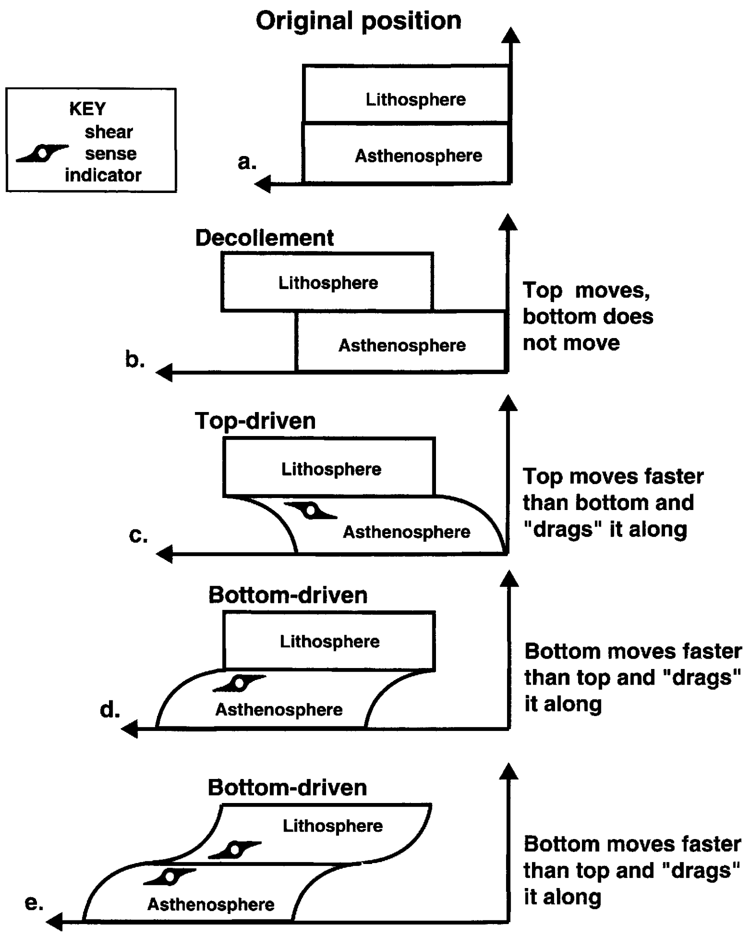

Fig. 5. Vertical, cross-sectional views of the relation between crustal and mantle deformation. The indicator represents an imaginary, initially vertical line that changes orientation with deformation (a loose line). The crust moves the same amount in all cases, but the relation between the upper crust and the mantle changes. Detachments (**b**) cause no fabric and are not consistent with the coincidence of crust and mantle deformation. Top-driven systems (**c**) produce the opposite sense of shear from bottom-driven systems (**d**,**e**). The lower crust can be involved (**e**), or not (**d**), in a bottom-driven system. Bottom-driven systems are expected to be the norm in orogenic belts. Modified from Tikoff *et al.* (2002).

movements ultimately result from deep-mantle processes. Bottom-driven systems do not require particular wavelengths of deformation, as the deformation does not proceed by amplification of instabilities. Rather, deformation is semi-continuous, an observation which is matched in many orogenic zones (e.g. Beavan & Haines 2001).

Top-driven systems

The Pacific Ocean lithosphere–asthenosphere (Fig. 2) and other ocean basins are potentially a good example of a top-driven tectonic system. In this case, the movement of the oceanic lithosphere may be governed by boundary forces affecting the edges of the plates (ridge push or slab pull), which affects the flow of the asthenosphere. Available seismic anisotropy data imply a velocity gradient between the plate and the mesosphere, and it is assumed that the higher-viscosity mesosphere moves more slowly. Regardless, as the lithosphere is pulled toward a subduction zone, the gradual variation in viscosity that causes the rheological layering of the lithosphere and asthenosphere will lead to a wide zone of decoupling. Note that this top-driven system does not deform the oceanic crust away from the ridge. This rigidity probably results from the homogeneous nature of oceanic crust compared to continental crust.

Bottom-driven systems

The coincidence of upper crustal and upper mantle deformation in continental settings suggests that the processes in these two layers are coupled. Movement must ultimately result from mantle convection driven by thermal dissipation, and thus the likely outcome of coupled mantle and crustal deformation is that orogenic systems are bottom-driven (e.g. Molnar 1992).

The formation of fabrics in the lower crust is also consistent with a notion of partial attachment (Tikoff *et al.* 2002). Even complete attachments result in the formation of different fabric, as the lithospheric layers have differing rheologies. Complete décollements occur in Nature and require zones of mechanical decoupling, which are generally discrete (e.g. salt horizons in a thrust system). The ubiquitous occurrence of originally subhorizontal, lower crustal layering and structural indications of high strain (intrafolial folds, sheath folds) suggests mechanical communication between the upper crust and upper mantle. Consequently, not only is coupled surficial (upper crustal) and mantle deformation explained by clutch tectonics, but so is the formation of lower crustal layering (Tikoff *et al.* 2002).

The major question of what causes the flow patterns in orogenic zones remains. If one of the lithospheres involved in plate interaction is relatively strong, such as an oceanic or strong cratonal region, deformation will preferentially occur in the weaker region, which will eventually become a deformation zone. The effect of lithospheric roots (from cratons, magmatic arcs, etc.) is therefore to channel asthenospheric mantle flow. The three-dimensional flow in the mantle within these deformation zones is thus controlled by relative plate movement. This movement, in turn, causes pressure gradients in the mantle and lithospheric thickness variations. Finally, part of the simple shear component parallel to the plate margin is probably an intrinsic part of the global (convective) mantle flow. It is clearly obtained in convection models, provided that the plate boundaries are characterized by a very efficient strain softening.

Implications for tectonics

Based on surficial crustal movements, interpretation of lithospheric and asthenospheric mantle fabric, and inferences of lower crustal deformation, we propose three-dimensional models for obliquely convergent, transcurrent and obliquely divergent boundaries. These are shown in block diagrams in Figure 6. We first discuss the strain patterns (e.g. Fossen & Tikoff 1993; Fossen *et al.* 1994) and the resultant LPO (e.g. Tommasi *et al.* 1999) that we would expect if the deformation were homogeneous. We then compare these predictions to the observations of crustal deformation and shear-wave splitting.

We wish to emphasize that these models are not strictly based on lithospheric strength profiles. Although these strength profiles are the basis for many tectonic models, they are extrapolations of laboratory data that may or may not be useful guides to rock behaviour at geological conditions. While strength profiles are widely utilized, our approach is to relax these criteria to put together an alternative, empirically based model. Additionally, we do not explicitly incorporate other models, such as lower crustal channel flow (e.g. Royden *et al.* 1997), which are derived principally from the strength profiles.

Transcurrent boundaries (Fig. 6a)

Wrench deformation makes a very simple prediction about the formation of fabrics. The material is essentially deformed within a simple shear zone, with the shear zone oriented vertically and parallel to the plate margin. In this setting, plane strain fabrics are expected to develop. Foliation is vertical and lineation is horizontal (foliation is defined by the maximum and intermediate axes of finite strain; lineation by the maximum axis of finite strain). Although both fabrics are initially oriented at a 45° to the shear plane, they rotate into parallelism with increasing finite strain (e.g. Lin & Williams 1992). The fabric in the mantle that corresponds to this style of deformation depends on the exact process of formation of the LPO (Fig. 1; e.g. point distributions v. girdle patterns). Regardless of the model chosen, strong shear-wave splitting from this LPO is predicted for vertical foliation and horizontal lineation (Fig. 1). The predictions of Tommasi *et al.* (1999) for wrench deformation are shown in Figure 7.

Transcurrent boundaries have a very straightforward kinematic relation with respect to lithospheric coupling. Major strike-slip faults within the continental lithosphere cut the entire crust and continue into the mantle lithosphere (Stern & McBride 1997; Hole *et al.* 1998). Fast polarization directions are typically subparallel or at a low angle to major active faults, including the San Andreas fault (California; Özalaybey &

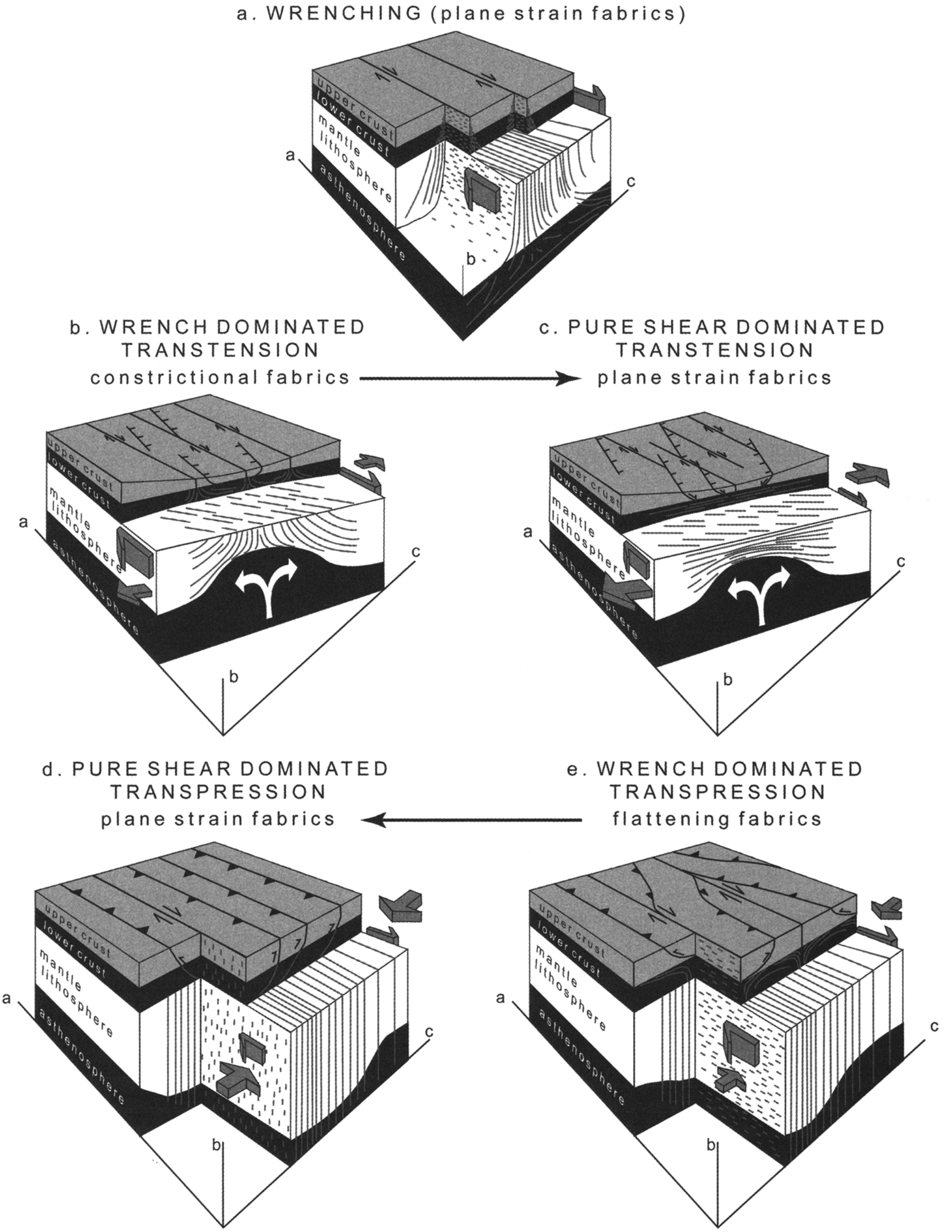

Fig. 6. Block diagrams of idealized deformation of the lithosphere. Wrench deformation (**a**) occurs in transcurrent plate boundaries and results in plane strain fabrics. Oblique divergence results in wrench-dominated transtension (**b**) or pure shear-dominated transtension (**c**), both of which result in constrictional fabrics. Pure shear-dominated transtension causes horizontal foliations. Pure shear-dominated transpression (**d**) and wrench-dominated transpression (**e**) result from oblique plate convergence. Both are associated with flattening fabrics. Pure shear-dominated transpression should result in vertical lineations, which cause low amounts of shear-wave splitting in the absence of lateral extrusion. Deformation that is dominantly divergent or convergent (e.g. pure shear-dominated) will tend towards plane strain fabrics.

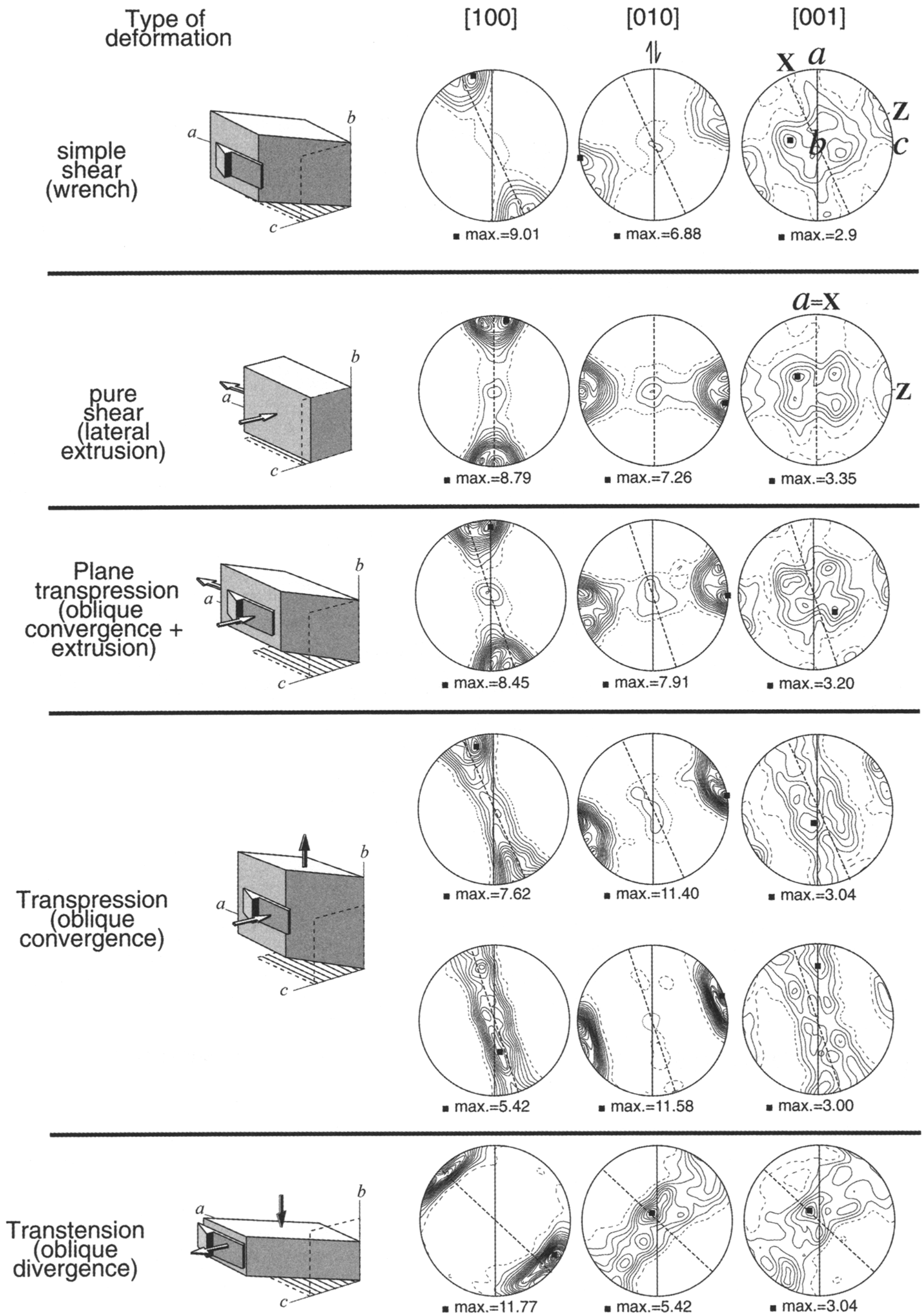

Fig. 7. Deformation types and the orientation of crystallographic axes of olivine, from predictions of a polycrystalline plasticity model valid for high-temperature (>900 °C) deformation in the mantle. The deformation types are shown as blocks on the left side of the diagram. Lower-hemisphere, equal-area stereonets are shown for the olivine crystallographic axes for 1000 grains contoured at 1% intervals. The black box shows the maximum LPO in each stereonet. Two predictions of LPO are shown for transpression, distinguishing wrench-dominated (top – long axis of finite strain ellipsoid is horizontal) and pure shear-dominated (bottom – long axis of finite strain ellipsoid is vertical). In general, olivine LPO is subparallel to the finite strain axes. Modified from Tommasi *et al.* (1999).

Savage 1995), El Pilar fault (Venezuela; Russo *et al.* 1996), Kunlun fault (Tibet; McNamara *et al.* 1994) and Altyn Tagh (Tibet; Herquel *et al.* 1995). Note that, in the case of the San Andreas fault, only the topmost of two layers of anisotropic material is oriented at a low angle to the San Andreas fault (Özalaybey & Savage 1995). For the San Andreas and New Zealand cases, the mantle fabric appears to rotate towards parallelism with the boundary as one approaches the fault. This observation suggests that the deformation gradient is highest under the fault, but that deformation in the mantle occurs broadly under these plate boundaries.

The same is true for the crustal deformation, as all of the transcurrent motions of these boundaries are not accommodated on the major, plate-boundary faults. Diffuse crustal deformation accommodating transcurrent motion was proposed for the San Andreas system by Jamison (1991) and Teyssier & Tikoff (1998), and is observed geodetically and structurally for the South Island of New Zealand (e.g. Beavan & Haines 2001; Little *et al.* 2002). Similar patterns are inferred from major, ancient strike-slip faults, such as the Great Glen fault (Scotland; Helffrich 1995) and strike-slip zones in the Appalachians (Barruol *et al.* 1997). As addressed earlier, this fabric survives, and potentially even controls, subsequent continental break-up (Vauchez *et al.* 1997; Tommasi & Vauchez 2001).

Divergence (Fig. 6b, c)

Oblique divergence will typically result in transtensional deformation, provided that a straight margin exists with a consistent oblique divergence movement direction. Transtension deformations typically lead to constrictional fabrics, although the exact nature of the fabric depends on the angle of oblique divergence and the amount of deformation (Fossen & Tikoff 1993; Fossen *et al.* 1994). Wrench-dominated transtension occurs for angles of oblique divergence less than 20°. Except settings that are within a few degrees from pure transcurrent motion, wrench-dominated transtension will result in very constrictional deformation. For pure shear-dominated transtension and higher angles of oblique divergence, the deformation will start to approach plane strain controlled by the divergent component of motion. The lineation is parallel to the oblique movement direction and not the shear zone boundary. Foliation is vertical for low finite strain and low angles of oblique divergence. For any oblique divergence direction greater than 20°, the foliation is always horizontal (e.g. Fossen *et al.* 1994). The LPO of olivine tracks these directions well (Fig. 7), as determined by a polycrystalline plasticity model valid for high-temperature (>900 °C) mantle deformation (Tommasi *et al.* 1999). In general, less shear-wave splitting is expected for obliquely divergent settings, because of the horizontal foliation (Fig. 1).

Divergence in continental lithosphere results in extensional or transtensional deformation, depending on the angle of oblique divergence. Mantle deformation shows characteristic fabrics with the fast split wave polarized oblique to the regional structural trend. The Rio Grande (Sandvol *et al.* 1992) and East Africa (Kenya; Gao *et al.* 1997) rifts both display this pattern. Lithospheric thinning may follow the structural expression of the rift, as demonstrated in Kenya (Achauer *et al.* 1994). Upper crustal deformation responds to this deformation by undergoing a combination of strike-slip and normal faulting (e.g. Doser & Yarwood 1991). The similarity of upper crustal deformation patterns is closely consistent with experimental models of bottom-controlled deformation (Withjack & Jamison 1986).

Polycrystalline plasticity models predict that olivine LPO developed in response to a transtensional deformation will be oblique to the rift trend, giving rise to a seismic anisotropy signal characterized by fast split shear wave polarized in a direction oblique to the rift elongation (Tommasi *et al.* 1999). This is consistent with the orientation of the shear-wave splitting data observed in the continental rifts. In our model (Fig. 6b, c), upwelling and outward flowing asthenosphere provides the basal drag to cause the formation of fabrics in the lithospheric mantle. As regions experiencing oblique divergence typically have high heat flow, such as the Basin and Range region of the western United States, it is assumed that only the uppermost part of the mantle forms an LPO. This occurs because high temperatures tend to favour diffusional creep, which does not produce an LPO.

We have not included passive rifting and/or orogenic collapse in the above model, despite the fact that these processes undoubtedly exist. Thickening of the crust and lithosphere inevitably introduces thermo-mechanical effects, such as thermal relaxation and time-dependent heating. These effects would act to decrease the coupling between the crust and the upper mantle (Vanderhaeghe & Teyssier 2001). These extensional systems may undergo top-driven collapse (e.g. Axen *et al.* 1998), bottom-driven collapse, or some combination, with the variation occurring on both a spatial and temporal basis (e.g. Rey *et al.* 2002; Tikoff *et al.* 2002). The connection between these processes and mantle flow requires more study.

Convergence (Fig. 6d, e)

Convergence plate boundaries include oceanic–oceanic, continental–oceanic, or continental–continental settings. We will concentrate on oceanic–continental and continental–continental settings. Oblique convergence results in transpressional deformation. Transpression causes flattening fabrics, which approach plane strain (pure shear) at very high angles of convergence. Foliation is always vertical, although lineation can be horizontal or vertical. Horizontal lineations, which result in strong shear-wave splitting, occur for an oblique convergence direction less than 20° and for low strains (e.g. Fossen & Tikoff 1993; Fossen *et al.* 1994). The lineation starts at less than 45° to the shear zone boundary (plate boundary) and rotates into parallelism with the shear zone boundary at higher finite strain. Polycrystalline plasticity models (Tommasi *et al.* 1999) show good agreement between olivine LPO and finite strain axes (Fig. 7). Consequently, strong shear-wave splitting is predicted for the case of horizontal lineations. For the pure shear end-member, however, the vertical lineations provide very low to no shear-wave splitting.

Convergent settings show the largest difference between inferred mantle fabric from seismology and crustal deformation. In most orogenic zones, reverse faulting and associated folding show large amounts of crustal contraction perpendicular to the trend of the belt. In contrast, shear-wave splitting is generally perpendicular to the maximum shortening direction, for both neotectonic (Tien Shan, Wolfe & Vernon 1998) and ancient examples (Hercynian, Bormann *et al.* 1993; Ribeira belt, Heinz *et al.* 2003). Note, however, that some measurements are parallel to the maximum shortening direction in the above cases. From these data, mantle deformation is inferred to extend material perpendicular to the contraction direction and parallel to the trend of the belt. As indicated by Tommasi *et al.* (1999), this pattern cannot result from a pure shear deformation in the mantle in the plane of the shortening direction. Pure shear would create a vertical long axis which is incompatible with the large (>1 s) shear-wave splitting observed in these areas.

Ways of interpreting the data include: (1) simple shear deformation; (2) pure shear deformation acting in a horizontal plane (lateral extrusion); or (3) a combination of the two (Fig. 4). Geodetic and structural studies are not consistent with large amounts of strike-slip movement in many foreland fold and thrust belts. In the Himalayas, shear-wave splitting increases as one approaches the major strike-slip faults, including the Kunlun and Altyn Tagh (Fig. 4). The other possibility is coaxial deformation, lateral extrusion, which elongates material parallel to the strike of the fold and thrust belt. (We use 'lateral extrusion' to indicate a pure shear that both elongates and shortens material in a horizontal plane, although other kinematic possibilities for lateral extrusion are possible.) Lateral extrusion would explain the nearly exact perpendicular relation between shear-wave splitting and crustal contraction.

Lateral extrusion requires some level of partial detachment (i.e. clutch tectonics). The shear-wave splitting data indicate that the upper mantle is undergoing contractional flow below the thrust belt, in a similar direction to the crustal deformation. However, because of the different boundary conditions, the direction of extension is different for the crust and mantle. Because of the free surface of the Earth, the extension direction is upward and crustal deformation is characterized as reverse faulting. In the mantle, material cannot move downward easily, as it must displace other material. Therefore, the mantle moves laterally. Alternatively, both simple shear and a component of lateral extrusion act together (plane transpression).

If extrusion tectonics is applicable to the Himalayan collision (e.g. Tapponnier *et al.* 2002), it is worth considering the role of mantle flow, in a bottom-driven system, and its effect on crustal deformation. The crustal deformation is only partially coupled from this extrusion, and accommodates more contractional deformation. A normal fault system occurs over most of the Tibetan plateau, which strikes north–south (parallel to the contraction direction) (Armijo *et al.* 1986; Yin *et al.* 1999). These normal faults are potentially recording a component of the extension deformation imposed by the extruding mantle flow in addition to lower crustal flow (Fig. 4). However, it is useful to remember that strain is a result of displacement gradient. This requires that the displacement from mantle extrusion increases from west to east (or, possibly, although less likely, from east to west) across Tibet. While the above discussion does not prove that the Himalayas are a bottom-driven system, it does indicate that a bottom-driven system is kinematically viable.

Strike-slip partitioning and homogeneous mantle deformation

Strike-slip faults, which parallel the trend of the orogen, occur in most mountain belts. Although described originally for obliquely convergent arc settings (e.g. Fitch 1972), strike-slip faulting also occurs in continental collisions, such as the Himalayas, with dominantly convergent motion (e.g. strike-slip partitioning; Teyssier *et al.* 1995).

If the upper crust is coupled to the mantle, the zones of strike-slip motion in the upper crust must represent zones of strong displacement gradients in the mantle. The physical experiments of Richard & Cobbold (1990) are a good analogy for this deformation. In these experiments, a layer of sand overlays a viscous silicone layer and the deformation was controlled by the bottom of the experiment. The sand developed a strike-slip fault immediately above maximum gradient of displacement in the underlying silicone. The sand on either side of the fault was deformed, often with reverse faults, but which accommodated a component of wrenching.

If the upper mantle partitioned deformation at a scale smaller than a seismic wave, one would expect shear zones parallel to the plate margin accommodating the transcurrent motion and lithons between the shear zones accommodating the contraction (Fig. 8). As the shear waves would preferentially travel through the larger lithons, this would cause fabric parallel to the major faults. The absence of this pattern (e.g. South Island of New Zealand) indicates that the mantle does not partition deformation into discrete high-strain zones. Rather, the correspondence of crustal deformation and shear-wave splitting requires that the mantle deforms in a relatively homogeneous manner.

Strike-slip partitioning, and most other crustal features in orogenic zones, may thus depend more on the mantle flow than local strength heterogeneities in the crust. The kinematic connection between movement in the mantle and crust may occur despite the major difference in the style of deformation: the upper crust deforms by faulting while the mantle deforms by crystal-plastic deformation. Although plate-margin-parallel, strike-slip faults are locally necessary to accommodate mantle flow, and they are not capable of accommodating contraction or extension. Consequently, large regions of contractional or extensional deformation, exhibiting reverse or normal faults, must accommodate the remaining part of the imposed mantle displacement. Different types of faults (e.g. strike-slip and reverse) must coexist to accommodate brittle deformation driven by movement of a ductile substrate. Consequently, the concept of a single regional stress direction that typifies an orogen is not compatible with a bottom-driven system. The simple relation between stress and flow may occur exclusively in the mantle, while the crust deforms passively in response to an imposed basally driven displacement field. To use the vernacular, the interesting physics may all be in the mantle while the crust rides along.

Absolute plate motion (APM) v. relative plate motion (RPM)

A potentially productive approach is to study the difference between absolute plate motion (APM)

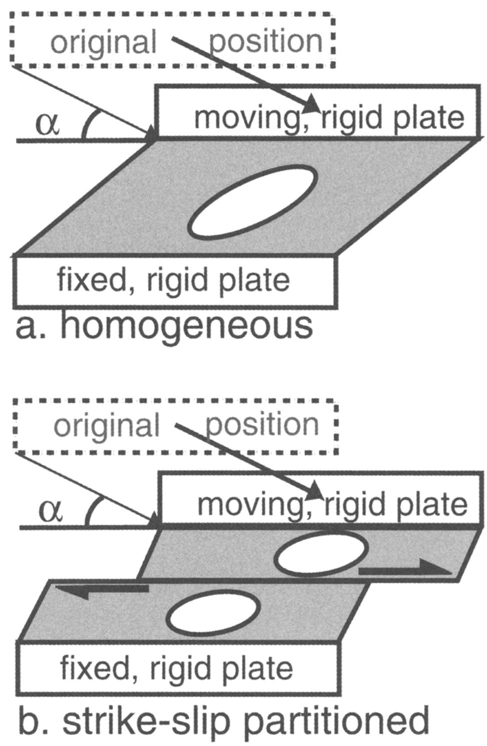

Fig. 8. (**a**) Orientation of finite strain for homogeneous and partitioned transpression. α is the angle of oblique convergence. The magnitude of finite strain is proportional to the amount of LPO and, therefore, to the amount of shear-wave splitting. (**b**) Partitioned deformation at any scale less than a seismic wave (e.g. shear bands) will tend to reduce the amount of splitting and the angle between the maximum splitting and the boundary. The correspondence between crustal deformation and shear-wave splitting (e.g. Little *et al.* 2002) indicates that this scale of deformation partitioning does not occur in the mantle.

and relative plate motion (RPM) for plate margins with large transcurrent components of motion. The APM is fixed with respect to hotspots. The San Andreas system in central California and El Pilar system in Trinidad are a particularly useful comparison (Fig. 9), because of their difference in APM. Both margins record largely transcurrent motion and similar amounts of displacement (e.g. Crowell, 1966; Speed 1985). The San Andreas fault, defined as the plate boundary between the North American and the Pacific plates, moves southwestward in an absolute reference frame. Consequently, the San Andreas fault moves approximately perpendicular to its strike relative to the mantle (Figs 3 & 9). Essentially, the plate boundary between the North American and Pacific plate moves westward, overrunning its old position in the asthenosphere. In contrast, the plate boundary between the South American and Caribbean plates, reflected by the El Pilar fault of Venezuela and its equivalent in Trinidad, is fixed in an absolute reference frame (Figs 3 & 8).

There is a discernible effect of APM on the deformation fabric, as reflected in the shear-wave splitting observed in both places. The San Andreas system has low splitting values, with delay travel times only up to 1.25 s (Hartog & Schwartz 2001). In fact, models for interpreting shear-wave splitting in this area require a two-layer anisotropy model, in which only the upper layer reflects a fabric at a low angle to the San Andreas fault (e.g. Özalaybey & Savage 1995; Hartog & Schwartz 2001). In general, within California, there is a gradual rotation in the polarization of fast split shear waves from NE–SW in easternmost California to east–west in central California. This pattern can be interpreted as a large-scale drag in the mantle, reflecting a change from olivine LPO oriented parallel to the APM to that reflecting the San Andreas fault.

Trinidad/Venezuela has relatively large splitting (Russo *et al.* 1996), with delay travel times of $\sim$2 s. The large splitting indicates that both the lithospheric mantle and part of the asthenospheric mantle are pervasively deformed. The data also show alignment subparallel ($\sim$5–8° obliquity) to the Caribbean/South American plate boundary, unlike other transcurrent plate boundaries (San Andreas, New Zealand), where the splitting is at a higher angle to the major transcurrent faults. Because the Caribbean/South American plate boundary is fixed in an absolute reference frame, we interpret the near-parallelism and high delay times to reflect the higher finite strains recorded along this boundary.

Therefore, it appears that relative motion is not the only factor in the development of mantle fabric. Rather, there are also important structural implications and differences in mantle fabric resulting from the absolute plate motion. For instance, the Caribbean/South American plate boundary is a relatively narrow and well-defined boundary. There are essentially two plates that have relative movement and a $\sim$100 km wide deformation zone between them. The strong fabrics and narrow deformational zone may result from the fixed position

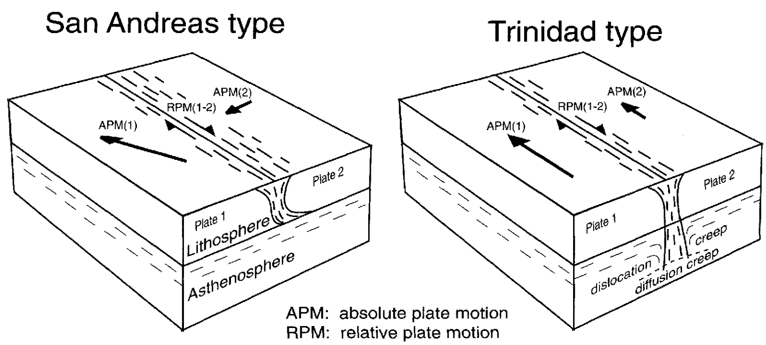

Fig. 9. The role of absolute plate motion in mantle deformation, as shown by a comparison of the San Andreas and Trinidad systems. Both systems have approximately transcurrent relative motion. The San Andreas system moves WSW, with respect to a fixed mantle framework. Consequently, the lithospheric wrenching deformation (e.g. fault system) is moving with respect to the asthenosphere. This may result in low amounts of splitting and very heterogeneous deformation. In contrast, crustal movement in Trinidad is parallel to the absolute plate motion and the plate boundary does not move in a fixed mantle framework. The parallelism of shear-wave splitting and the narrowness ($\sim$100 km) of the deformation zone are a possible result of the lithospheric boundary being coincident with an asthenospheric boundary.

of the plate boundary in the mantle. In contrast, the Pacific/North America plate boundary in central California is wide and complicated. Instead of two plates, there is also the Sierra Nevada–Great Valley microplate that is moving to the northwest, although at a decreased rate. This complexity may result from the southwestward movement of the San Andreas fault system, in an absolute motion framework.

Conclusions

The similarity of deformation patterns in the upper crust (structural reconstruction, geodetic data, etc.) and upper mantle (shear-wave splitting, azimuthal anisotropy of Pn waves, etc.) indicate that these lithospheric layers are, at least, partially coupled. Crustal rocks in these deforming zones are hypothesized to be moving on a thin and flowing mantle, inferred from seismic attenuation studies. This deforming mantle controls orogenesis. Applying the clutch model – partial attachment between lithospheric layers – allows us to address three-dimensional models of convergent, transcurrent and divergent plate margins, for both crustal and mantle deformation. The history of the plate margin and the absolute plate motion are critical, as both influence the mantle fabric and overlying crustal structures.

BT and CT would like to thank the public library in Black River Falls, Wisconsin, for providing a meeting room, in which the first version of this paper was outlined. The authors would like to thank Shun Karato for numerous conversations about olivine deformation. BT wishes to thank Scott Giorgis and Eric Horsman for work on the manuscript that allowed it to be submitted at all.

References

ABRAMSON, E.H., BROWN, J.M., SLUTSKY, L.J. & ZAUG, J. 1997. The elastic constants of San Carlos Olivine to 17 GPa. *Journal of Geophysical Research*, **102**, 12253–12263.

ACHAUER, U., GLAHN, A., *et al.* 1994. New ideas on the Kenya Rift based on the inversion of the combined dataset of the 1985 and 1989/90 seismic tomography experiments. *In*: PRODEHL, C., KELLER, G.R. & KHAN, M.A. (eds) Crustal and upper mantle structure of the Kenya Rift. *Tectonophysics*, **236**, 305–329.

AMATO, A., CHIARABBA, C. & SELVAGGI, G. 1997. Crustal and deep seismicity in Italy (30 years after). *Annali di Geofisica*, **40**, 981–993.

ARMIJO, R., TAPPONNIER, P., MERCIER, J.-L. & HAN, T.L. 1986. Quaternary extension in southern Tibet; field observations and tectonic implications. *Journal of Geophysical Research*, **91**, 13803–13872.

AXEN, G.J., SELVERSTONE, J., BYRNE, T. & FLETCHER, J.M. 1998. If the strong crust leads, will the weak crust follow? *GSA Today*, **8**, 1–8.

BAI, Q., MACKWELL, S.J. & KOHLSTEDT, D.L. 1991. High-temperature creep of olivine single crystals, 1. Mechanical results for buffered samples. *Journal of Geophysical Research*, **96**, 2441–2463.

BARRUOL, G. & KERN, H. 1996. Seismic anisotropy and shear-wave splitting in lower-crustal and upper-mantle rocks from the Ivrea Zone: experimental and calculated data. *In*: MAINPRICE, D. & VAUCHEZ, A. (eds), Dynamics of the subcontinental mantle; from seismic anisotropy to mountain building. *Physics of the Earth and Planetary Interiors*, **95**, 175–194.

BARRUOL, G., HELFFRICH, G. & VAUCHEZ, A. 1997. Shear wave splitting around the northern Atlantic; frozen Pangaean lithospheric anisotropy? *In*: MAINPRICE, D., BOUDIER, F. & BOUCHEZ, J.L. (eds) The Adolphe Nicolas volume. *Tectonophysics*, **279**, 135–148.

BEAVAN, J. & HAINES, J. 2001. Contemporary horizontal velocity and strain rate fields of the Pacific–Australian plate boundary zones through New Zealand. *Journal of Geophysical Research*, **106**, 741–770.

BEN ISMAEL, W. & MAINPRICE, D. 1998. An olivine fabric database: an overview of upper mantle fabrics and seismic anisotropy. *Tectonophysics*, **296**, 145–158.

BORMANN, P., BURGHART, P.T., MAKEYEVA, L.I. & VINNIK, L.P. 1993. Teleseismic shear-wave splitting and deformations in central Europe. *Physics of the Earth and Planetary Interiors*, **78**, 157–166.

BOSTOCK, M.G. & CASSIDY, J.F. 1995. Upper mantle stratigraphy beneath the southern Slave Craton. *Canadian Journal of Earth Science*, **34**, 577–587.

BRACE W.F. & KOHLSTEDT D.L. 1980. Limits on lithospheric stress imposed by laboratory experiments. *In:* HANKS, T.C. & RALEIGH, C.B. (eds), Magnitude of deviatoric stresses in the Earth's crust and uppermost mantle. *Journal of Geophysical Research*, **85**, 6248–6252.

BURG, J.P., DAVY, P. & MARTINOD, J. 1994. Shortening of analogue models of the continental lithosphere; new hypothesis for the formation of the Tibetan Plateau. *Tectonics*, **13**, 475–483.

BYSTRIKY, M., KUNZE, K., BURLINI, L. & BURG, J.P. 2000. High shear strain of olivine aggregates: rheological and seismic consequences. *Science*, **290**, 1564–1567.

CALVERT, A., SANDVOL, E., *et al.* 2000. Geodynamic evolution of the lithosphere and upper mantle beneath the Alboran region of the western Mediterranean: constraints from travel time tomography. *Journal of Geophysical Research*, **105**, 10871–10898.

CARLSON, R.L. 1995. A plate cooling model relating rates of plate motion to the age of the lithosphere at trenches. *Geophysical Research Letters*, **22**, 1977–1980.

CARTER, N.L. & AVÉ LALLEMANT, H.G. 1970. High temperature flow of dunite and peridotite. *Geological Society of America Bulletin*, **81**, 2180–2202.

CHASTEL, Y.B., DAWSON, P.R., WENK, H.R. & BENNETT, K. 1993. Anisotropic convection with implications for the upper mantle. *Journal of Geophysical Research*, **98**, 17757–17771.

CHRISTENSEN, J.N., ROSENFELD, J.L. & DEPAOLA, D.J. 1989. Rates of tectonometamorphic processes from rubidium and strontium isotopes in garnet. *Science*, **244**, 1465–1469.

CHRISTENSEN, N.I. 2002. Continental mantle seismic anisotropy: a new look at the Twin Sisters massif. *Tectonophysics*, **355**, 163–170.

CHRISTENSEN, N.I. & MOONEY, W.D. 1995. Seismic velocity structure and composition of the continental crust; a global view. *Journal of Geophysical Research*, **100**, 9761–9788.

CROWELL, J.C. 1966. Displacements along the San Andreas fault, California. *Annales Academia Scientiarum Fennicae, Series A3: Geologica–Geographica*, **90**, 119–125.

DOSER, D.I. & YARWOOD, D.R. 1991. Strike-slip faulting in continental rifts; examples from Sabukia, East Africa (1928), and other regions. *In:* Gangi, A.F. (ed) World rift systems. *Tectonophysics*, **197**, 213–224.

DUNLAP, W.J., HIRTH, G. & TEYSSIER, C. 1997. Thermomechanical evolution of a ductile duplex. *Tectonics*, **16**, 983–1000.

ENDERLE, U., MECHIE, J., SOBOLEV, S. & FUCHS, K. 1996. Seismic anisotropy within the uppermost mantle of southern Germany. *Geophysical Journal International*, **125**, 747–767.

FITCH, T.J. 1972. Plate convergence, transcurrent faults, and internal deformation adjacent to Southeast Asia and the Western Pacific. *Journal of Geophysical Research*, **77**, 4432–4460.

FOSSEN, H. & TIKOFF, B. 1993. The deformation matrix for simultaneous simple shearing, pure shearing and volume change, and its application to transpression–transtension tectonics. *In:* CASEY, M., DIETRICH, D., FORD, M., WATKINSON, J. & HUDLESTON, P.J. (eds) The geometry of naturally deformed rocks. *Journal of Structural Geology*, **15**, 413–422.

FOSSEN, H., TIKOFF, B. & TEYSSIER, C. 1994. Strain modeling of transpression and transtensional deformation. In: KRILL, A.G. & LIPPARD, S.J. (eds) Strike-slip tectonics: Proceedings of the 10th TSGS conference. *Norsk Geologisk Tidsskrif*, **74**, 134–145.

GAO, S., DAVIS, P.M., *et al.* 1997. SKS splitting beneath continental rift zones. *Journal of Geophysical Research*, **102**, 22781–22797.

GIORGIS, S., MARKLEY, M., and TIKOFF, B. 2004. Vertical-axis rotation of rigid crustal blocks driven by mantle flow. *In*: GROCOT, J., MCCAFFREY, K.J.W., TAYLOR, G. & TIKOFF, B. (eds) *Vertical Coupling and Decoupling in the Lithosphere*. Geological Society, London, Special Publications, **227**, 83–99.

GOSCOMBE, B. 1992. High-grade reworking of central Australian granulites: Part 1, Structural evolution. *Tectonophysics*, **204**, 361–399.

HARTOG, R. & SCHWARTZ, S.Y. 2001. Depth-dependent mantle anisotropy below the San Andreas Fault system; apparent splitting parameters and waveforms. *Journal of Geophysical Research*, **160**, 4155–4167.

HATZFELD, D., KARAKOSTAS, V., *et al.* 2000. Microseismicity and faulting geometry in the Gulf of Corinth (Greece). *Geophysical Journal International*, **141**, 438–456.

HEARN T.M. 1996. Anisotropic Pn tomography in the Western United States. *Journal of Geophysical Research*, **101**, 8403–8414.

HEARN T.M. 1999. Uppermost mantle velocities and anisotropy beneath Europe. *Journal of Geophysical Research*, **104**, 15123–15139.

HEINTZ, M., VAUCHEZ, A., ASSUMPCAO, G., BARRUOL, G. & EGYDIO-SILVA, M. 2003. Shear wave spilling in SE Brazil: an effect of active on fossil upper mantle flow, or both? *Earth and Planetary Science Letters*, **211**, 79–95.

HELFFRICH, G. 1995. Lithospheric deformation inferred from teleseismic shear wave splitting observations in the UK. *Journal of Geophysical Research*, **100**, 18195–18204.

HERQUEL, G., WITTLINGER, G. & GUILBERT, J. 1995. Anisotropy and crustal thickness of Northern-Tibet: new constraints for tectonic modelling. *Geophysical Research Letters*, **22**, 1925–1928.

HESS, H.H. 1964. Seismic anisotropy of the uppermost mantle under oceans. *Nature*, **203**, 629–631.

HOLE J.A., BEAUDOIN, B.C. & HENSTOCK, T.J. 1998. Wide-angle seismic constraints on the evolution of the deep San Andreas plate boundary by Mendocino triple junction migration. *Tectonics*, **17**, 802–818.

HOLT, W.E. 2000. Correlated crust and mantle strain fields in Tibet. *Geology*, **28**, 67–70.

IMBER, J., HOLDSWORTH, R.E. & BUTLER, C.A. 2001. A reappraisal of the Sibson–Scholz fault zone model: the nature of the frictional to viscous ('brittle–ductile') transition along a long-lived, crustal-scale fault, Outer Hebrides, Scotland. *Tectonics*, **20**, 601–624.

JAMES, D.E. & ASSUMPCAO, M. 1996. Tectonic implications of S-wave anisotropy beneath SE Brazil. *Geophysical Journal International*, **126**, 1–10.

JAMISON, W.R. 1991. Kinematics of compressional fold development in convergent wrench terranes. *Tectonophysics*, **190**, 209–232.

JORDAN, T.H. 1975. The continental tectosphere. *Reviews of Geophysics and Space Physics*, **13**, 1–12.

KAMINSKI, E. & RIBE, N.M. 2001. A kinematic model for recrystallization and texture development in olivine polycrystals. *Earth and Planetary Science Letters*, **189**, 253–267.

KENNEDY, L.A., RUSSEL, J.K. & KOPYLOVA, M.G. 2002. Mantle shear zones revisited: the connection between the cratons and mantle dynamics. *Geology*, **30**, 419–422.

KLOSKO, E., WU, F., *et al.* 1999. Upper mantle flow in the New Zealand region from seismic anisotropy. *Geophysical Research Letters*, **26**, 1497–1500.

KOHLSTEDT, D.L., EVANS, B. & MACKWELL, S.J. 1995. Strength of the lithosphere: constraints imposed by laboratory experiments. *Journal of Geophysical Research*, **100**, 17587–17602.

LAVE, J., AVOUAC, J.P., LACASSIN, R., TAPPONNIER, P. & MONTAGNER, J.P. 1996. Seismic anisotropy beneath Tibet; evidence for eastward extrusion of the Tibetan lithosphere? *Earth and Planetary Science Letters*, **140**, 83–96.

LAY, T. & WALLACE, T.C. 1995. *Modern Global Seismology*. Academic Press, San Diego, CA.

LIN, S. & WILLIAMS, P.F. 1992. The geometrical relationship between the stretching lineation and the movement directions of shear zones. *Journal of Structural Geology*, **14**, 491–497.

LITTLE, T.A., SAVAGE, M.K. & TIKOFF, B. 2002. Relationship betweem crustal finite strain and seismic anisotropy in the mantle, Pacific–Australia plate boundary zone, South Island, New Zealand. *Geophysical Journal International*, **151**, 160–169.

MACKWELL, S.J., KOHLSTEDT, D.L. & PATERSON, M.S. 1985. The role of water in the deformation of olivine single crystals. *Journal of Geophysical Research*, **90**, 11319–11333.

MARGHERITI, L., NOSTRO, C., AMATO, A. & COCCO, M. 1996. Seismic anisotropy; an original tool to understand the geodynamic evolution of the Italian Peninsula. *In:* MANTOVANI, E. (ed.) Geodynamics of the Mediterranean region and its implications for seismic and volcanic risk. *Annali di Geofisica*, **40**, 759–769.

MARSON-PIDGEON, K.A. & SAVAGE, M.K. 1997. Frequency-dependent anisotropy in Wellington, New Zealand. *Geophysical Research Letters*, **24**, 3297–3300.

MCKENZIE, D. & JACKSON, J. 1983. The relationship between strain rates, crustal thickening, palaeomagnetism, finite strain and fault movements within a deforming zone. *Earth and Planetary Science Letters*, **65**, 182–202.

MCNAMARA, D.E., OWENS, T.J., SILVER, P.G. & WU, F.T. 1994. Shear wave anisotropy beneath the Tibetan Plateau. *Journal of Geophysical Research*, **99**, 655–665.

MELE, G., ROVELLI, A., SEBER, D., HEARN, T.M. & BARAZANGI, M. 1998. Compressional velocity structure and anisotropy in the uppermost mantle beneath Italy and surrounding regions. *Journal of Geophysical Research*, **103**, 12529–12543.

MOCHIZUKI, K., KASAHARA, J., SATO, T., SHINOHARA, M. & HIRATA, N. 1997. Seismic refraction tomography and its application in an experiment in the Tsushima Basin, Japan Sea. *Geophysical Exploration*, **50**, 179–195.

MOLNAR, P. 1992. Brace–Goetze strength-profiles, the partitioning of strike-slip and thrust faulting at zones of oblique convergence, and the stress–heat flow paradox of the San Andreas fault. *In:* EVANS, B. & WONG, T.-F. (eds) *Fault Mechanics and Transport Properties of Rocks*. Academic Press, New York, 435–459.

MOLNAR, P., ANDERSON, H.J., *et al.* 1999. Continuous deformation versus faulting through the continental lithosphere of New Zealand. *Science*, **286**, 516–519.

MONTAGNER, J.-P. & TANIMOTO, T. 1990. Global anisotropy in the upper mantle inferred from the regionalization of phase velocities. *Journal of Geophysical Research*, **95**, 4797–4819.

MONTAGNER, J.-P. & TANIMOTO, T. 1991. Global upper mantle tomography of seismic velocities and anisotropies. *Journal of Geophysical Research*, **96**, 20337–20351.

MOORE, M., ENGLAND, P. & PARSONS, B. 2002. Relation between surface velocity field and shear-wave splitting in the South Island of New Zealand. *Journal of Geophysical Research*, **107**, doi: 10.1029/2000JB000093.

NISHIMURA, C.E. & FORSYTH, D.W. 1988. Rayleigh wave phase velocities in the Pacific with implications for azimuthal anisotropy and lateral heterogeneities. *Journal of Geophysical Research*, **94**, 479–501.

NISHIMURA, C.E. & FORSYTH, D.W. 1989. The anisotropic structure of the upper mantle in the Pacific. *Geophysical Journal of the RAS, DGG,* and EGS, 96, 203–229.

OKAL, E.A. & TALANDIER, J. 1997. T waves from the great 1994 Bolivian deep earthquake in relation to channeling of S wave energy up the slab. *Journal of Geophysical Research*, **102**, 27421–27437.

OLDOW, J.S., BALLY, A.W. & AVÉ LALLEMANT, H.G. 1990. Transpression, orogenic float, and lithospheric balance. *Geology*, **18**, 991–994.

ÖZALAYBEY, S. & SAVAGE, M.K. 1995. Shear-wave splitting beneath western United States in relation to plate tectonics. *Journal of Geophysical Research*, **100**, 18135–18149.

PHAKEY, P., DOLLINGER, G. & CHRISTIE, J. 1972. Transmission electron microscopy of experimentally deformed olivine crystals. *In:* Flow and fracture of rocks. *Geophysical Monograph*, **16**, 117–138.

PLOMEROVA, J., BABUSKA, V. & HORALEK, J. 1998. Seismic anisotropy and velocity variations in the mantle beneath the Saxothuringicum–Moldanubicum contact in Central Europe. *In:* PLOMEROVA, J., LIEBERMANN, R.C. & BABUSKA, V. (eds) Geodynamics of lithosphere and Earth's mantle: seismic anisotropy as a record of the past and present dynamic processes. *Pure and Applied Geophysics*, **151**, 365–394.

PLOMEROVA, J., KOUBA, D. & BABUSKA, V. 2002. Mapping the lithosphere–asthenosphere boundary through changes in surface-wave anisotropy. *Tectonophysics*, **358**, 175–186.

RAITT, R.W., SHOR, G.G., FRANCIS, T.J.G. & MORRIS, G.B. 1969. Anisotropy of the Pacific upper mantle. *Journal of Geophysical Research*, **74**, 3095–3109.

REY, P., VANDERHAEGHE, O. & TEYSSIER, C. 2002. Gravitational collapse of continental crust: definitions, regimes, mechanisms and modes. *Tectonophysics*, **342**, 435–449.

RIBE, N.M. & YU, Y. 1991. A theory for plastic deformation and textural evolution of olivine polycrystals. *Journal of Geophysical Research*, **96**, 8325–8335.

RICHARD, P. & COBBOLD, P. 1990. Experimental insights into partitioning fault motions in continental convergent wrench zones. *In:* BOCCALETTI, M. & NUR, A. (eds) Active and recent strike-slip tectonics; selected papers from an international workshop. *Annales Tectonicae*, **4**, 35–44.

ROTH, E.G., WIENS-DOUGLAS, A., DORMAN, L.M., HILDEBRAND, J. & WEBB, S.C. 1999. Seismic attenuation tomography of the Tonga–Fiji region using phase pair methods. *Journal of Geophysical Research*, **104**, 4795–4809.

ROYDEN, L.H., BURCHFIEL, B.C., KING, R.W., WANG, E., CHEN, Z., SHEN, F. & LIU, Y. 1997. Surface deformation and lower crustal flow in eastern Tibet. *Science*, **276**, 788–790.

RUSSO, R.M. & OKAL, E.A. 1998. Shear wave splitting and upper mantle deformation in French Polynesia: evidence from small-scale heterogeneity related to the Society Hotspot. *Journal of Geophysical Research*, **103**, 15089–15107.

RUSSO, R.M., SILVER, P.G., FRANKE, M., AMBEH, W.G. & JAMES, D.E. 1996. Shear-wave splitting in northeast Venezuela, Trinidad, and the eastern Caribbean. *Physics of the Earth and Planetary Interiors*, **95**, 251–275.

SANDVOL, E., NI, J., OZALAYBEY, S. & SCHLUE, J. 1992. Shear-wave splitting in the Rio Grande Rift. *Geophysical Research Letters*, **19**, 2337–2340.

SAVAGE, M.K. 1999. Seismic anisotropy and mantle deformation; what have we learned from shear wave splitting? *Reviews of Geophysics*, **37**, 65–106.

SAVAGE, M.K. & SILVER, P.G. 1993. Mantle deformation and tectonics; constraints from seismic anisotropy in the western United States. *In:* MAINPRICE, D., VAUCHEZ, A. & MONTAGNER, J.P. (eds) Dynamics of the subcontinental mantle: from seismic anisotropy to mountain building. *Physics of the Earth and Planetary Interiors*, **78**, 207–227.

SCHOLZ, C.H. 1988. The brittle–ductile transition and the depth of seismic faulting. *Geologisches Rundschau*, **77**, 319–328.

SIBSON. R.H. 1977. Fault rocks and fault mechanisms. *Journal of the Geological Society of London*, **133**, 191–213.

SILVER, P.G. 1996. Seismic anisotropy beneath the continents: probing the depths of geology. *Annual Review of Earth and Planetary Sciences*, **24**, 385–432.

SILVER, P.G. & CHAN, W.W. 1991. Shear wave splitting and subcontinental mantle deformation. *Journal of Geophysical Research*, **96**, 16429–16454.

SILVER, P.G. & HOLT, W.E. 2002. The mantle flow field beneath western North America. *Science*, **295**, 1054–1058.

SPEED, R.C. 1985. Cenozoic collision of the Lesser Antilles Arc and continental South America and the origin of the El Pilar fault. *Tectonics*, **4**, 41–69.

STERN, T.A. & MCBRIDE, J.H. 1997. Seismic exploration of continental strike-slip zones. *In:* KLEMPERER, S.L. & MOONEY, W.D. (eds) Deep seismic profiling of the continents: I, General results and new methods. *Tectonophysics*, **286**, 63–78.

TAPPONNIER, P., ZHIQIN, X., ROGER, F., MEYER, B., ARNAUD, N., WITTLINGER, G. & JINGSUI, Y. 2002. Oblique stepwise rise and growth of the Tibetan Plateau. *Science*, **294**, 1671–1677.

TEYSSIER, C. & TIKOFF, B. 1998. Strike-slip partitioned transpression of the San Andreas fault system: a lithospheric scale approach. *In:* HOLDSWORTH, R.E., STRACHAN, R.A. & DEWEY, J.F. *Continental Transpression and Transtension Tectonics*. (eds) Geological Society, London, Special Publications, **135**, 143–158.

TEYSSIER, C., TIKOFF, B. & MARKLEY, M. 1995. Oblique plate motion and continental tectonics. *Geology*, **23**, 447–450.

TIKOFF, B. & GREENE, D. 1997. Stretching lineations in transpressional shear zones; an example from the Sierra Nevada Batholith, California. *Journal of Structural Geology*, **19**, 29–39.

TIKOFF, B., TEYSSIER, C. & WATERS, C.L. 2002. Clutch tectonics and partial attachment of lithospheric layers. *EUG Special Publication Series*, **1**, 93–117.

TOMMASI, A. & VAUCHEZ, A. 2001. Continental rifting parallel to ancient collisional belts: an effect of the mechanical anisotropy of the lithospheric mantle. *Earth and Planetary Science Letters*, **185**, 199–210.

TOMMASI, A., TIKOFF, B. & VAUCHEZ, A. 1999. Upper mantle tectonics: three-dimensional deformation, olivine crystallographic fabrics and seismic properties. *Earth and Planetary Science Letters*, **168**, 173–186.

TOMMASI, A., MAINPRICE, D., CANOVA, G. & CHASTEL, Y. 2000. Viscoplastic self-consistent and equilibrium-based modeling of olivine lattice preferred orientations: implications for the upper mantle seismic anisotropy. *Journal of Geophysical Research*, **105**, 7893–7908.

VANDERHAEGHE, O. & TEYSSIER, C. 2001. Crustal scale rheological transitions during late-orogenic collapse. *Tectonophysics*, **335**, 211–228.

VAN DER LEE, S. & NOLET, G. 1997. Seismic image of the subducted trailing fragments of the Farallon Plate. *Nature*, **386**, 266–269.

VAUCHEZ, A. & GARRIDO, C.J. 2001. Seismic properties of an asthenospherized lithospheric mantle: constraints from lattice preferred orientations in peridotite from the Ronda Massif. *Earth and Planetary Science Letters*, **192**, 235–249.

VAUCHEZ, A., TOMMASI, A. & EGYDIO-SANTOS, M. 1994. Self-indentation of a heterogeneous continental lithosphere. *Geology*, **22**, 967–970.

VAUCHEZ, A., BARRUOL, G. & TOMMASI, A. 1997. Why do continents break-up parallel to ancient orogenic belts? *Terra Nova*, **9**, 62–66.

VINNIK, L.P., FARRA, V. & ROMANOWICZ, B. 1989*a*. Azimuthal anisotropy in the Earth from observations of SKS at GEOSCOPE and NARS broadband stations. *Bulletin of the Seismological Society of America*, **79**, 1542–1558.

VINNIK, L.P., KIND, R., KOSAREV, G.L. & MAKEYEVA, L.I. 1989*b*. Azimuthal anisotropy in the lithosphere from observations of long-period S-waves. *Geophysics Journal International*, **99**, 549–559.

VINNIK, L.P., KRISHNA, V.G., KIND, R., BORMANN, P. & STAMMLER, K. 1994. Shear wave splitting in the records of the German Regional Seismic Network. *Geophysical Research Letters*, **21**, 457–460.

WENK, H.R. & TOME, C.N. 1999. Modeling dynamic recrystallization of olivine aggregates deformed in simple shear. *Journal of Geophysical Research*, **104**, 25513–25527.

WENK, H.R., BENNETT, K., CANOVA, G.R. & MOLINARI, A. 1991. Modelling plastic deformation of peridotite with the self-consistent theory. *Journal of Geophysical Research*, **96**, 8337–8349.

WITHJACK, M.O. & JAMISON, W.R. 1986. Deformation produced by oblique rifting. *Tectonophysics*, **126**, 99–124.

WOLFE, C.J. & SILVER, P.G. 1998. Seismic anisotropy of oceanic upper mantle; shear wave splitting methodologies and observations. *Journal of Geophysical Research*, **103**, 749–771.

WOLFE, C.J. & VERNON, F.L. 1998. Shear-wave splitting at central Tien Shan: evidence for rapid variation of anisotropic patterns. *Geophysical Research Letters*, **25**, 1217–1220.

YIN, A., KAPP, P.A., *et al.* 1999. Significant late Neogene east–west extension in northern Tibet. *Geology*, **27**, 787–790.

ZHANG, S. & KARATO, S. 1995. Lattice preferred orientation of olivine aggregates in simple shear. *Nature*, **375**, 774–777.

ZHANG, S., KARATO, S., FITZGERALD, J., FAUL, U. & ZHOU, Y. 2000. Simple shear deformation of olivine aggregates. *Tectonophysics*, **316**, 133–152.